

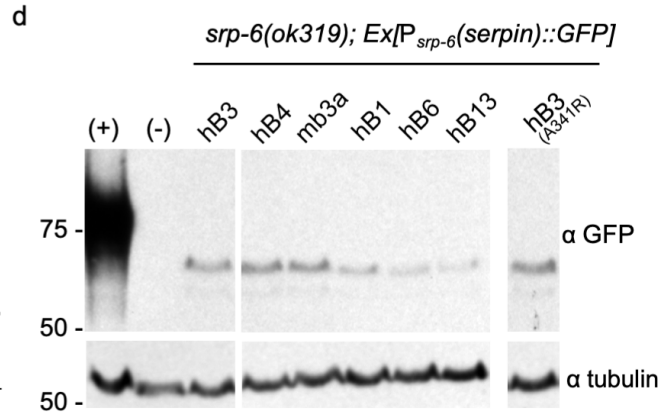
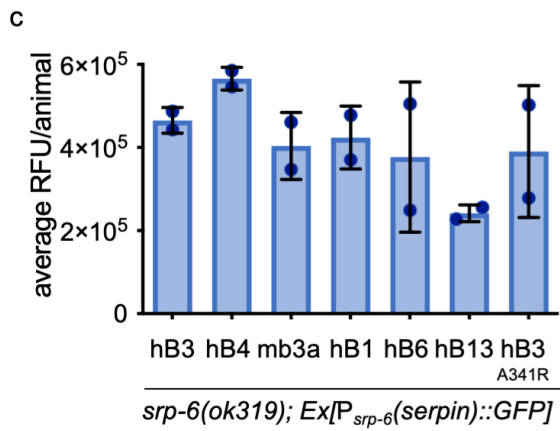
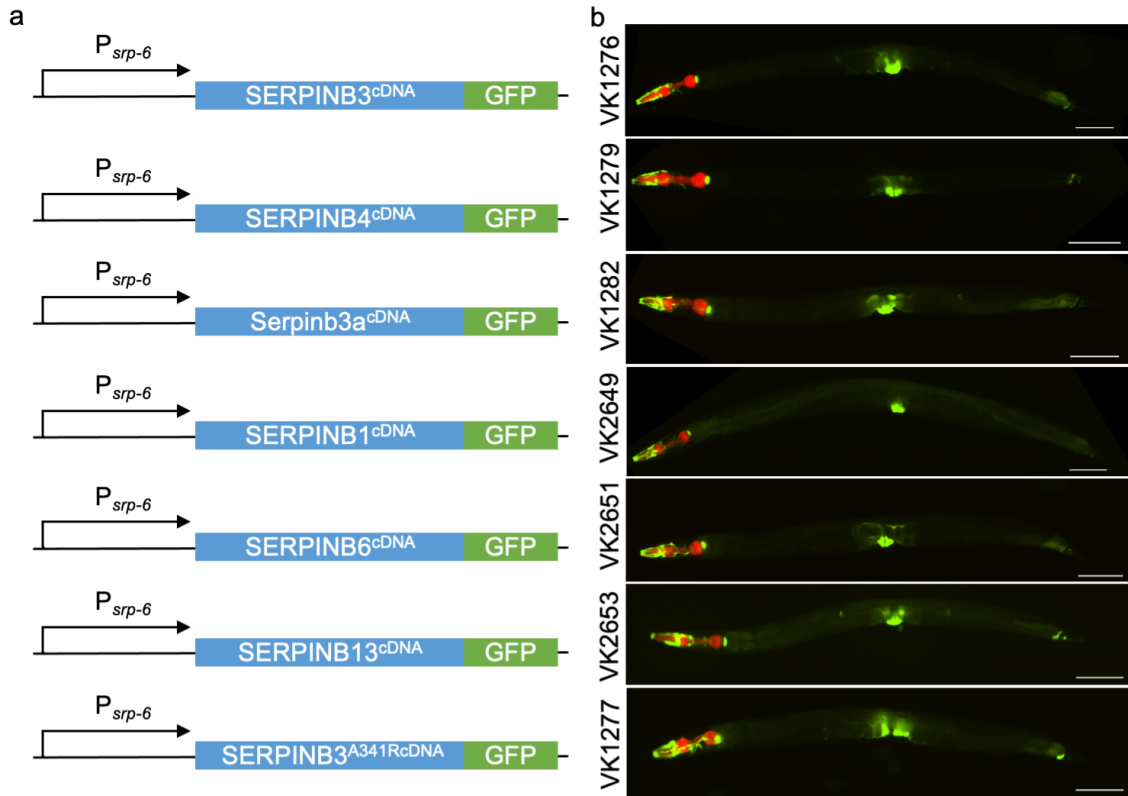
**LYSOPTOSIS IS AN EVOLUTIONARY CONSERVED CELL DEATH PATHWAY MODERATED BY
INTRACELLULAR SERPINS**

SUPPLEMENTARY INFORMATION:

Supplementary Tables and Figures

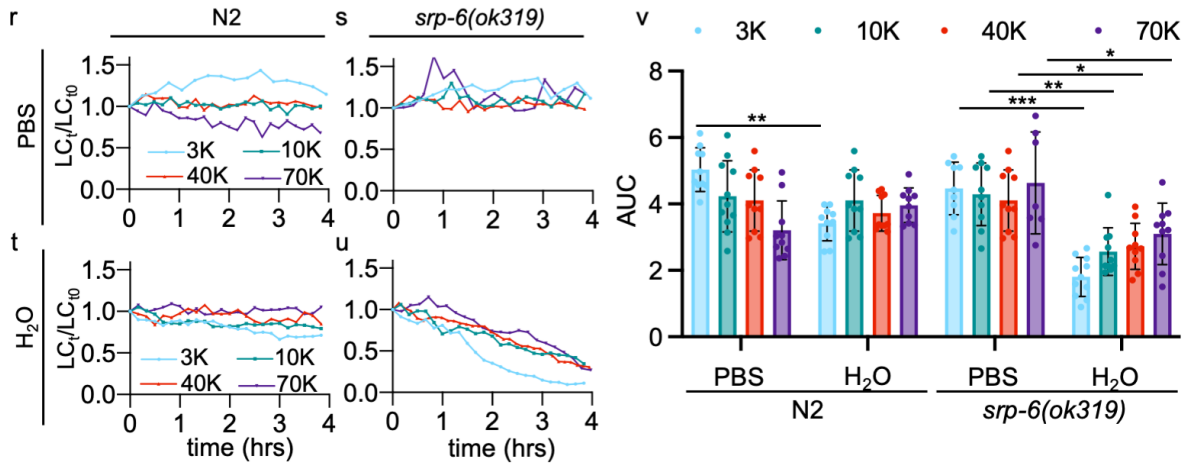
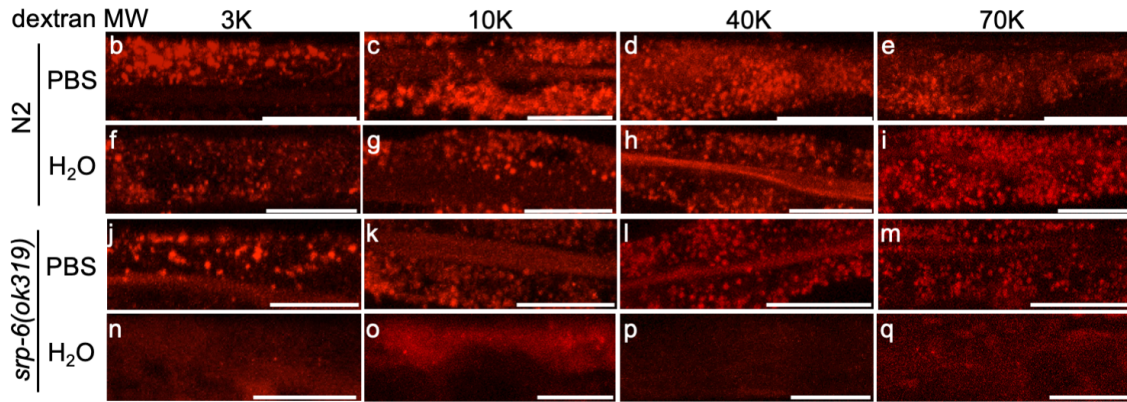
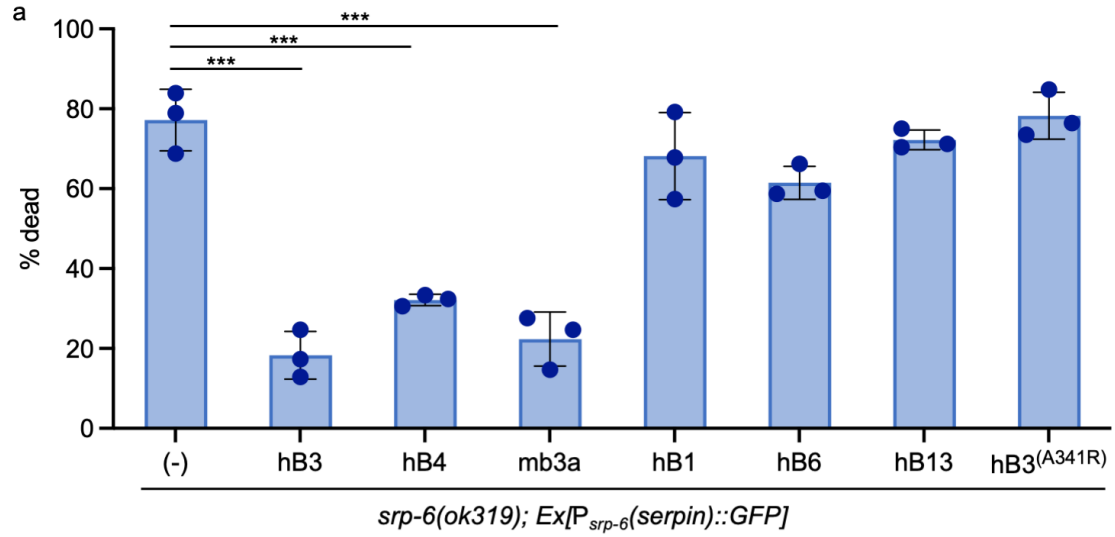
Cell line	% WT alleles	% gene indels
SW756 ^{B3-WT} ;CTSL-KO	11.6	88.4
SW756 ^{B3-KO} ;CTSL-KO	41.7	59.3

Table S1. NGS sequencing results for the cathepsin L knockout lines.



Supplementary Figure 1. Some mammalian serpins can replace the function of SRP-6 in *C. elegans*. (a) Schematic representation of the constructs used to generate the corresponding transgenic *C. elegans*. (b) Fluorescence microscopy of representative transgenic *C. elegans*, VK1276 (*srp-6(ok319);vkEx1276[P_{srp-6}SERPINB3^{cDNA}::GFP; P_{myo-2}mCherry]*) (hB3), VK1279 (*srp-6(ok319);vkEx1279[P_{srp-6}SERPINB4^{cDNA}::GFP; P_{myo-2}mCherry]*) (hB4), VK1282 (*srp-6(ok319);vkEx1282[P_{srp-6}Serpib3a^{cDNA}::GFP; P_{myo-2}mCherry]*) (mB3a), VK2649 (*srp-6(ok319);vkEx2649[P_{srp-6}SERPINB1^{cDNA}::GFP; P_{myo-2}mCherry]*) (hB1), VK2651 (*srp-6(ok319);vkEx2651[P_{srp-6}SERPINB6^{cDNA}::GFP; P_{myo-2}mCherry]*) (hB6), VK2653 (*srp-6(ok319);vkEx2653[P_{srp-6}SERPINB13^{cDNA}::GFP; P_{myo-2}mCherry]*) (hB13) and VK1277 (*srp-6(ok319);vkEx1276[P_{srp-6}SERPINB3^{(A341R)cDNA}::GFP; P_{myo-2}mCherry]*) (hB3^(A341R)) acquired using 488nm and 568nm excitation laser lines to excite GFP (green) and mCherry (red). (c) Approximately 15 animals of each of the transgenic lines were placed in individual wells of a 384-well plate over n = 2 wells and fluorescence was measured using the Cellinsight CX7 imaging plate reader (Thermo Fisher Scientific) in both the GFP (Ex 485 nm / Em 503-531 nm) and RFP (Ex 560 nm / Em 590-624 nm) channels. GFP and mCherry positive objects were identified by thresholding and the relative GFP fluorescence (RFU) was divided by the number of mCherry positive objects to generate the RFU / animal. The average RFU per animal was calculated over the multiple wells. The error bars represent the standard deviation from the mean. (d) Western blot analysis of the serpin transgene expression levels in the *C. elegans* transgenic lines. One hundred transgenic *C. elegans* were lysed in SDS-PAGE sample buffer with boiling for 5 mins and the proteins separated by SDS-PAGE prior to being transferred onto

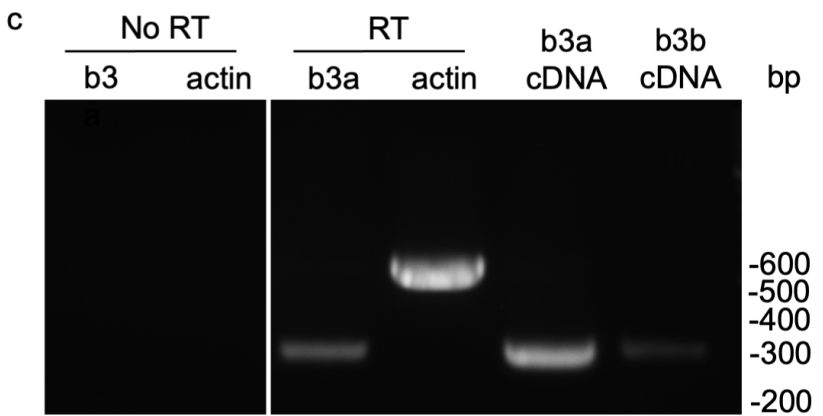
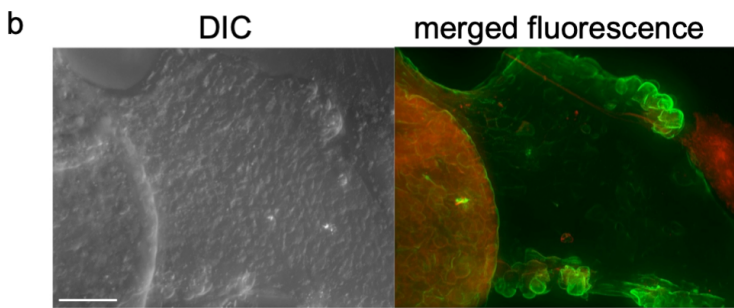
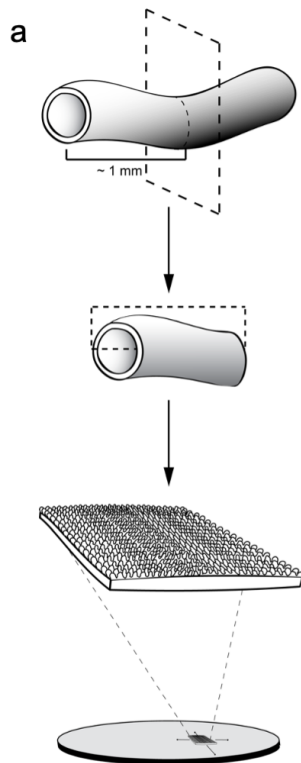
nitrocellulose. Transgene expression was then detected using anti-GFP mAb. Both N2 (-) and VK694 ($P_{nhx-2}SGFP::ATZ$; +) served as negative and positive western blotting controls. Loading of protein was determined by anti-tubulin mAb loading control.



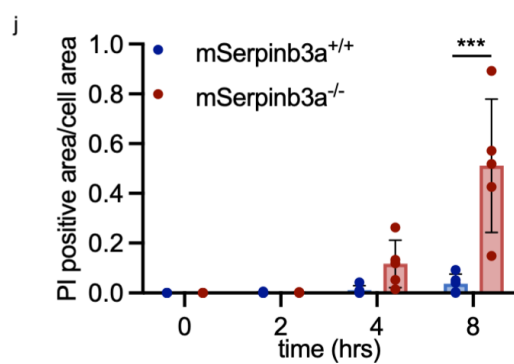
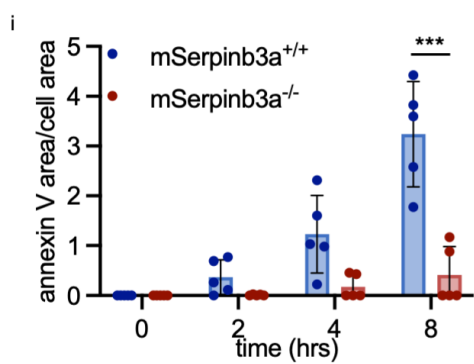
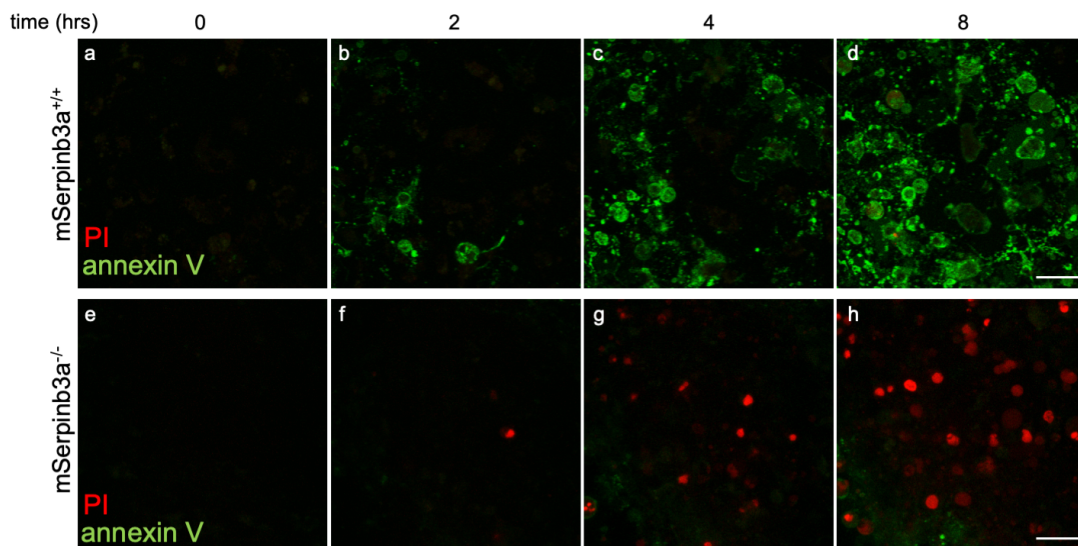
Supplementary Figure 2. Mammalian clade B serpins inhibit lysoptosis in

C. elegans. (a) Survival of *srp-6(ok319);P_{myo-2}mCherry* (-) and *srp-6(ok319);P_{myo-2}mCherry* transgenic lines expressing human *SERPINB3* (hB3, strain VK1276), human *SERPINB4* (hb4, strain VK1279), mouse *Serpib3a* (mB3a, strain VK1282), human *SERPINB1* (hB1, strain VK2649), human *SERPINB6* (hB6, strain VK2651), human *SERPINB13* (hB13, strain, VK2653) and human *SERPINB3* with an inactivating A341R mutation (hB3^(A341R)), strain VK1277) after exposure to hypotonic stress for 1 hour. Strains were selected for comparable levels of protein expression in mosaic animals (Fig. S1). Animals ($n \geq 20$) for each group were assayed on 3 separate days. The mean percent dead \pm the standard deviation (SD) from all three assays were plotted ($***P < 0.001$; two-tailed *t*-test). (b-v) Hypotonic stress induced lysosomal membrane permeabilization (LMP) in *srp-6(ok319)* *C. elegans*. (b-q). Representative maximum intensity projection confocal images of both wild-type (N2; b-i) and *srp-6(ok319)* *C. elegans* (j-q) labeled with Texas red conjugated dextrans of different molecular masses (kDa). Animals were exposed to PBS (b-e; j-m) or H₂O (f-i; n-q) and fluorescence (red; Ex 594nm/Em 620nm) was acquired by live animal confocal microscopy in XYZ planes approximately every 5 min over 4 hours in single animals ($n \geq 7$). The 4-hour time point is shown. Scale bars = 25 μ m. (r-u) Quantification of the different molecular mass dextrans (3 kDa (3K) (cyan), 10K (turquoise), 40K (red) and 70K (purple) in multiple animals ($n \geq 10$) of both wild-type N2 (r, t) and *srp-6(ok319)* (s, u) *C. elegans* exposed to PBS (r, s) or H₂O (t, u). The lysosomal count at each time point (LC_t) was normalized to the lysosome count at time point 0 (LC_{t0}) to generate the relative lysosomal abundance (LC_t/LC_{t0}). The average $LC_t/LC_{t0} \pm$ SD for each time point was plotted. Error

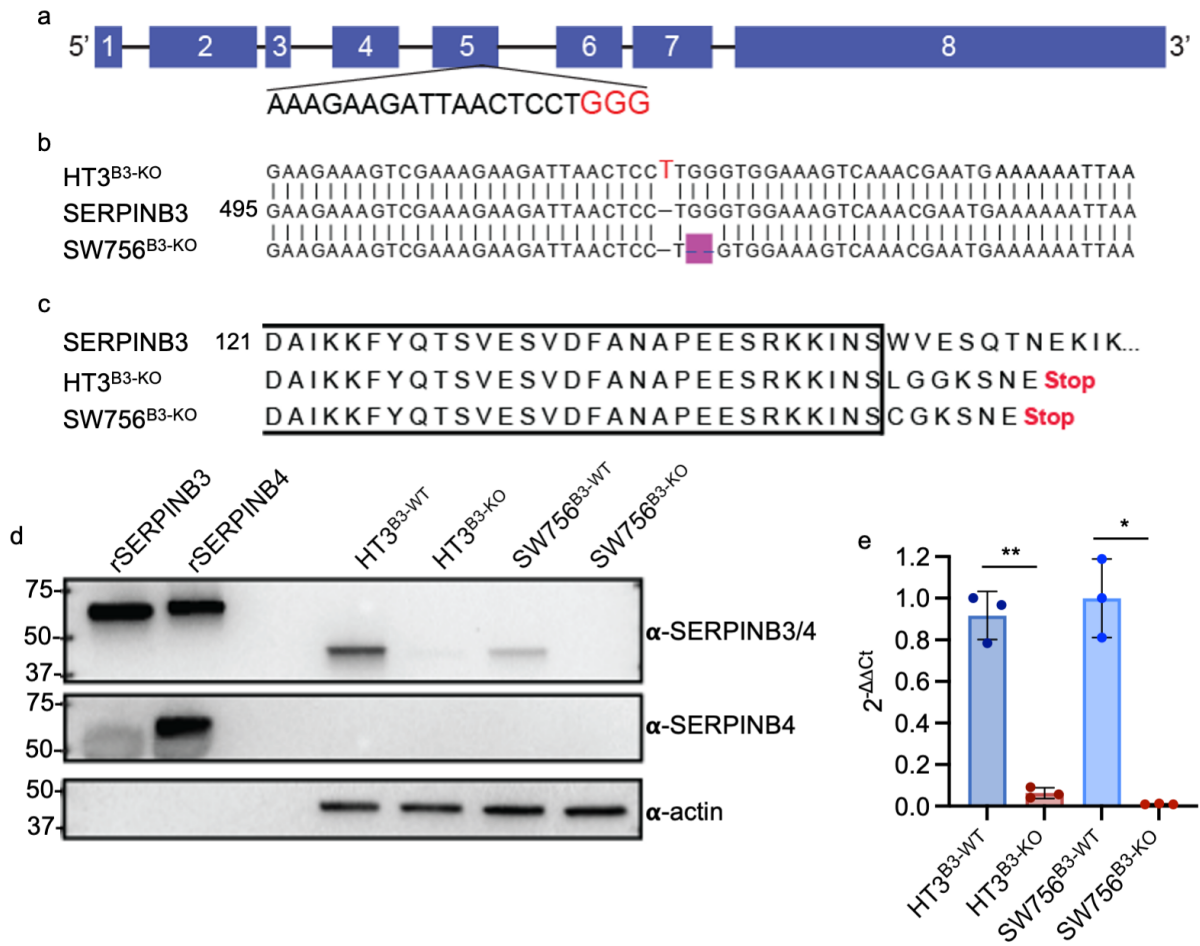
bars were not included to allow for visualization of the curves. A representative of 3 experiments is shown. (v) The area under the curve (AUC) was calculated for each dextran in each individual animal and the mean AUC \pm SD was plotted. The AUCs for the same molecular mass dextrans in the same *C. elegans* strains treated with PBS or H₂O were compared by 2-way ANOVA with Tukey multiple comparisons ($***P < 0.001$, $**P < 0.01$ and $*P < 0.05$). A representative experiment is shown.



Supplementary Figure 3. Establishment of FIEC cultures. (a) Schematic representation of the preparation of FIEC cultures for ex vivo imaging experiments. (b) Immunofluorescence of FIECs derived from *mSerpib3a^{+/+}* mice with a hamster monoclonal antibody that recognizes *Serpib3a* and *Serpib3b* (red) and a rabbit polyclonal antibody that recognizes the epithelial cell marker cytokeratin 8 (green). Primary antibodies were detected with Alexa Fluor 594 conjugated goat anti hamster and Alexa Fluor 488 conjugated goat anti-rabbit, respectively. (c) RT-PCR from FIECs derived from *mSerpib3a^{+/+}* mice with primers specific for mSerpib3a (expected product 302 bp) and actin (expected product 537 bp). No reverse transcriptase (No RT) reactions served as negative controls for the amplification of genomic DNA. Primer specificity was determined using plasmids containing the cDNA for *mSerpib3a* (+ve) and *mSerpib3b* (-ve).

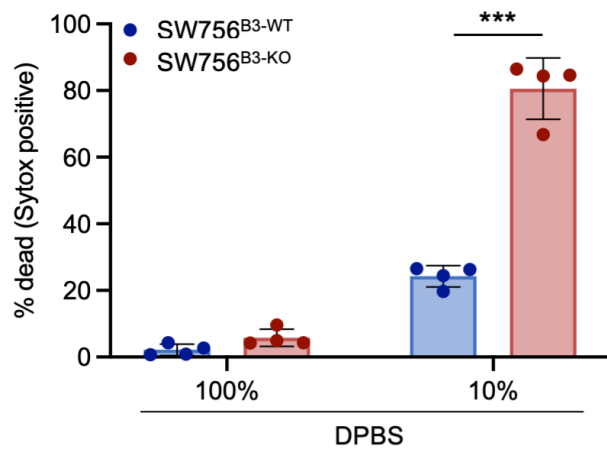


Supplementary Figure 4. mSerpib3a^{-/-} FIECs lose plasma membrane integrity early with staurosporine treatment. (a-h) Representative live cell time-lapse confocal fluorescence maximum intensity projections of mSerpib3a^{+/+} (a-d) or mSerpib3a^{-/-} (e-h) FIECs treated with 10 μ M staurosporine and stained with annexin V-FITC (green) and propidium iodide (red) at the indicated time points (hrs). Scale bar = 25 μ m. (i, j) Quantification of the annexin V area/cell area (i) and PI positive area/cell area (j) from multiple fields of view (n = 5) during the live-cell time lapse imaging at the indicated time points.

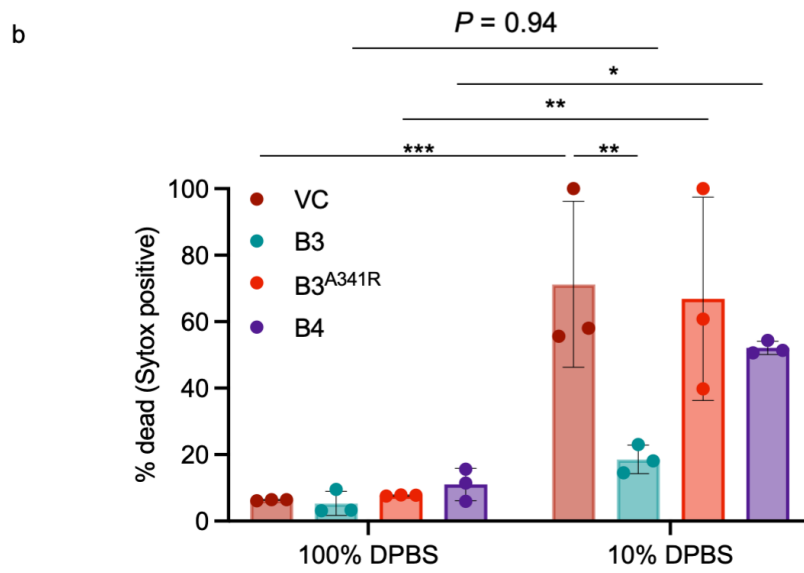
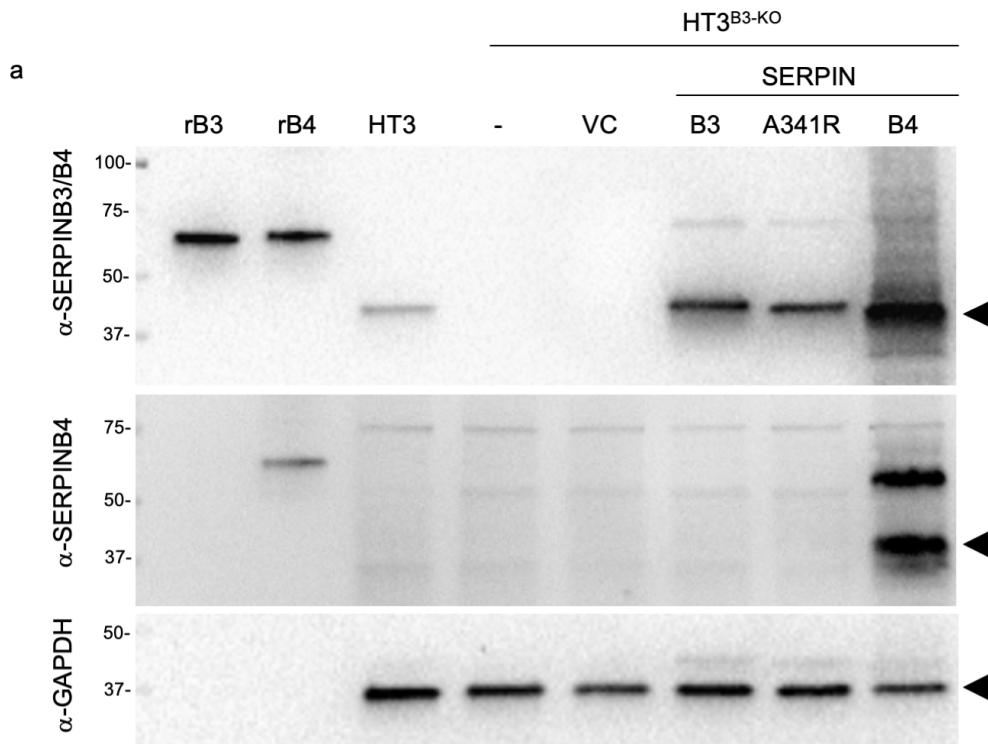


Supplementary Figure 5. CRISPR/Cas9 engineered tumor epithelial cell

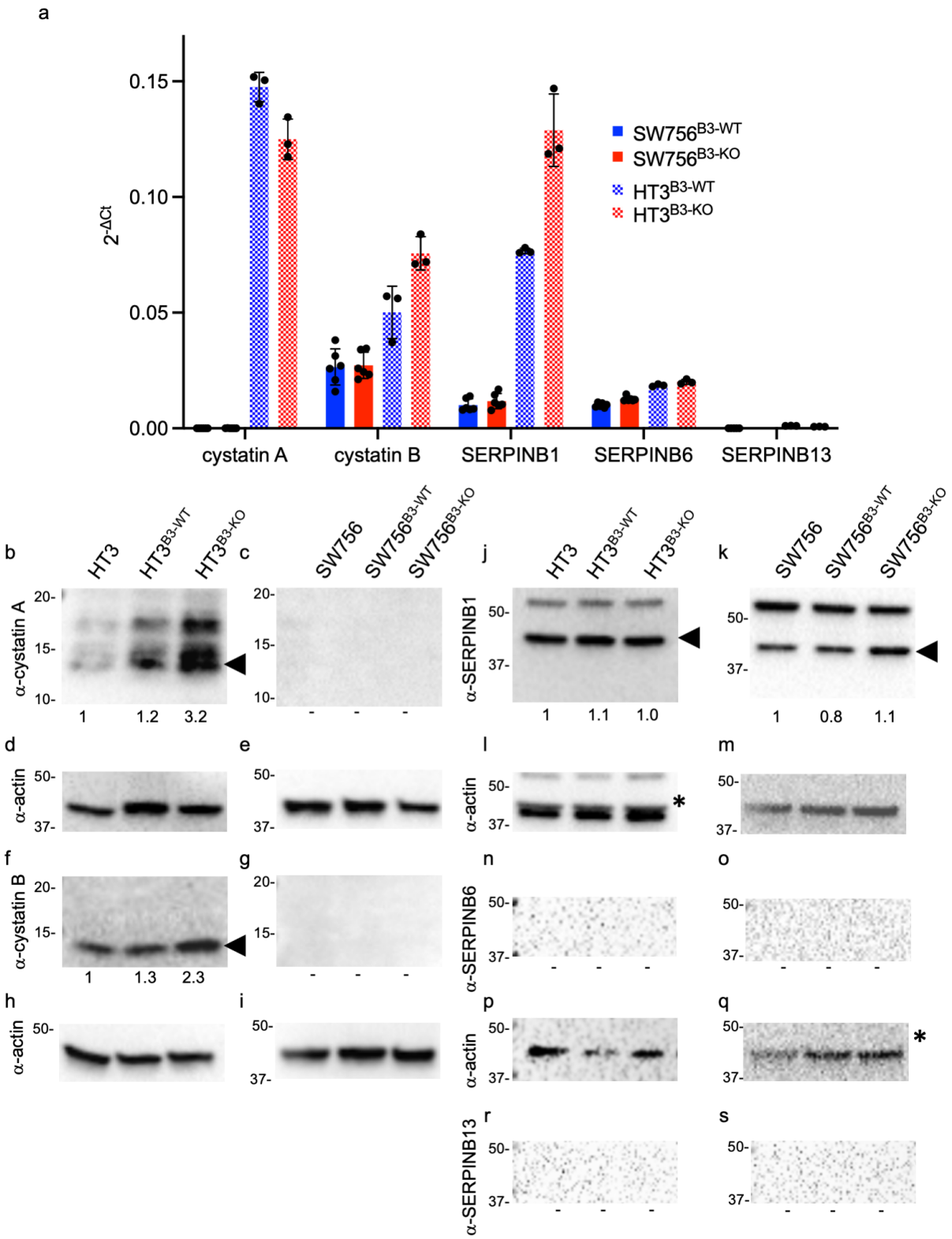
lines are null for SERPINB3. (a) Schematic representation of the genomic structure of human SERPINB3 with the gRNA target sequence shown between residues 432 and 451 within Exon 5 with the PAM site in red letters. (b) Sequence alignment of the wild-type human SERPINB3 reference sequence (Accession number NM_006919.3) with the cDNA sequences amplified by RT-PCR from HT3^{B3-KO} and SW756^{B3-KO} total RNA isolation. The HT3^{B3-KO} clone shows a single base pair (t) addition (red) whereas the SW756^{B3-KO} clone shows a 2-base pair indel (fuchsia), resulting in a frameshift prior to the reactive site loop. (c) ClustalW alignment of the predicted amino acid sequences of wild-type SERPINB3 (top line) and HT3^{B3-KO} (middle line) and SW756^{B3-KO} (bottom line) clones translated from amino acid 121. Both HT3^{B3-KO} and SW756^{B3-KO} clones show a premature stop codon at position 158 and 157, respectively. (d) Western blot analysis of protein levels of SERPINB3 in SW756 and HT3 control and B3 null cell lines using a monoclonal antibody (Novus) that recognizes both SERPINB3 and -B4 (α -SERPINB3/B4), 10C12 monoclonal antibody specific for SERPINB4 (α -SERPINB4) and actin (α -actin) control. Recombinant GST fusion SERPINB3 and -B4 (rhB3 and rhB4, respectively) serve as positive controls for the polyclonal antibody and both positive and negative controls for the monoclonal antibody. (e) Quantitative RT-PCR of SERPINB3 transcript levels (forward primer: CGCGGTCTCGTGCTATCTG, reverse primer: ATCCGAATCCTACTACAGCGG) for HT3^{B3-WT} and SW756^{B3-WT} (B3-WT) and the HT3^{B3-KO} and SW756^{B3-KO} clones (B3-KO) expressed in 2^{- $\Delta\Delta$ Ct} normalized to the wild-type. Note the dramatically reduced levels of transcript in the HT3^{B3-KO} cell line and the undetectable levels in the SW756^{B3-KO} clones.



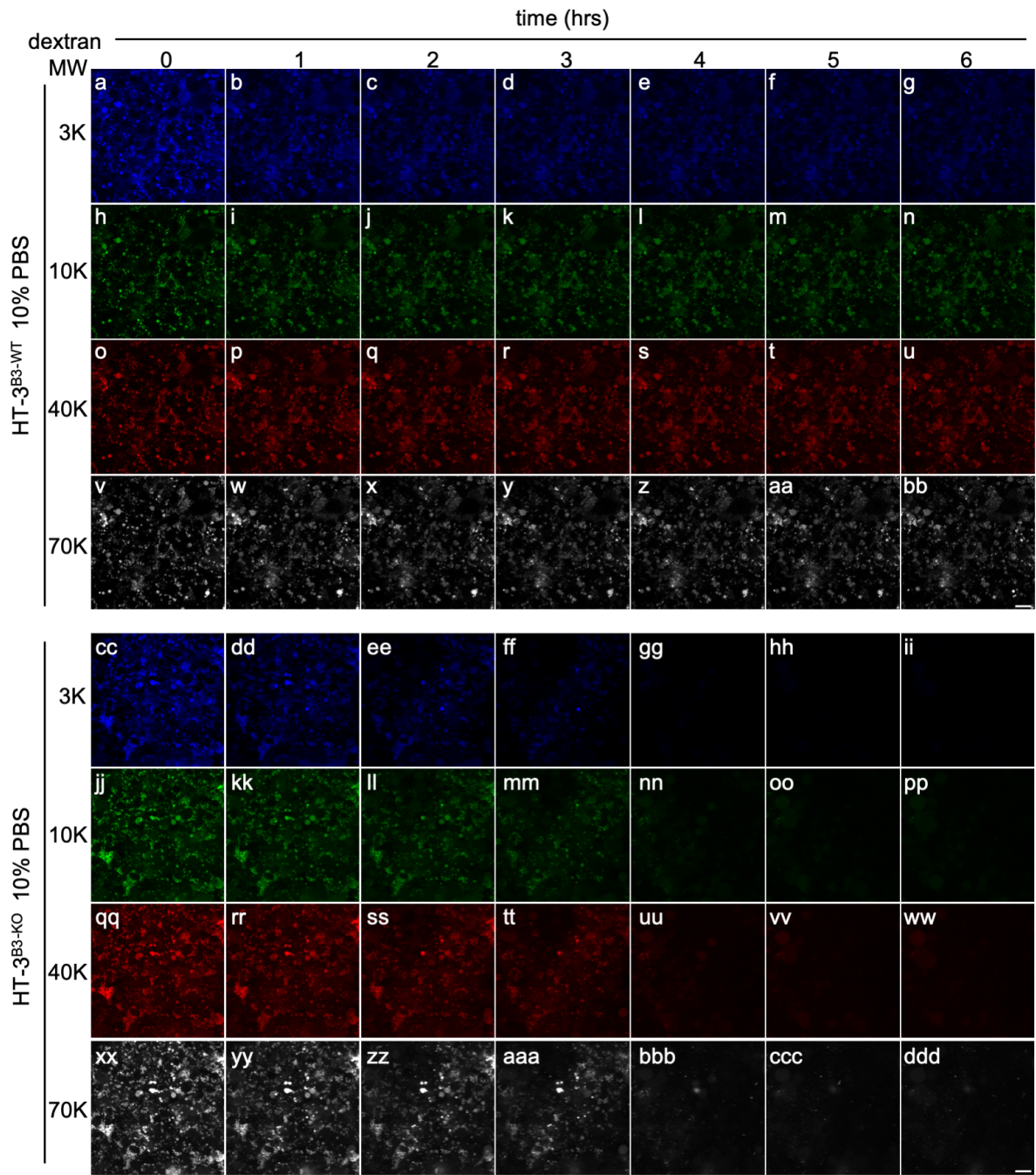
Supplementary Figure 6. Loss of SERPINB3 also sensitizes SW756 cells to hypotonic stress. A representative experiment showing SW756^{B3-WT} and SW756^{B3-KO} cell lines treated with either 100% or 10% DPBS in the presence of Sytox Green for 4 hours. Cells were then stained with H33342 before imaging. The percent dead was calculated as (# of Sytox™ positive/# of blue nuclei) × 100. The means ± SD were compared using a two-tailed *t*-test (***P* < 0.001).



Supplementary Figure 7. SERPINB3 rescues HT3^{B3-KO} cells from lysoptosis-like cell death. (a) Immunoblot analysis of cell lysates from HT3^{B3-WT} and HT3^{B3-KO} cells (-) nucleofected with empty vector (VC) or mammalian expression plasmids containing the cDNA for WT SERPINB3 (B3), SERPINB3^{A341R} (A341R) or SERPINB4 (B4) genes probed with a monoclonal antibody (Novus) that recognizes both SERPINB3 and SERPINB4 (α -SERPINB3/B4), 10C12 monoclonal antibody specific for SERPINB4 (α -SERPINB4) and actin (α -actin) control. Recombinant GST fusion SERPINB3 and -B4 (rB3 and rB4, respectively) serve as positive controls and both positive and negative controls for the monoclonal antibodies. (b) A representative experiment of the HT3 cells lines expressing empty vector control (VC; turquoise), SERPINB3 cDNA (B3; teal), the SERPINB3^{A341R} inactivating mutation cDNA (B3^{A341R}; red) and the SERPINB4 cDNA (B4; purple). Error bars represent the standard deviation from the mean. Statistical significance was analysed using a 2-way ANOVA with Tukey multiple comparisons (* $P < 0.05$; ** $P < 0.01$, *** $P < 0.001$). Note, there is no statistical difference between the 100% DPBS and 10% DPBS treated HT3^{B3-KO} expressing SERPINB3 ($P = 0.94$).

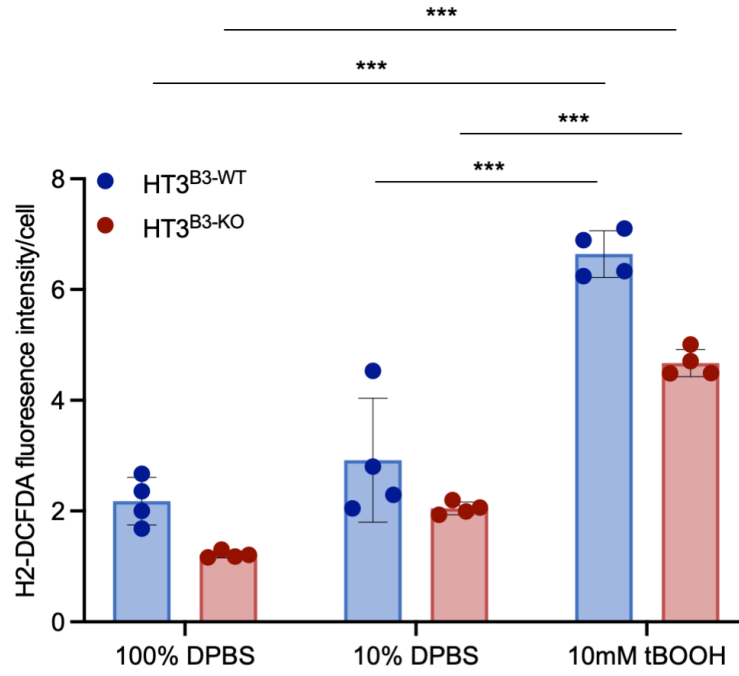


Supplementary Figure 8. Analysis of the expression of other functionally relevant protease inhibitors in SW756 and HT3 cell lines. Quantitative (q) RT-PCR (a) and western blot (WB) analysis (b-s) of cystatin A (qRT-PCR forward primer: GTACTTACTGGATAACCAGGTTGAC, reverse primer: AGTAGCCAGTTGAAGGAATCAG; WB primary antibody clone B-11, 1 in 1000 dilution Santa Cruz, sc-376759), cystatin B (qRT-PCR forward primer: GTACTTACTGGATAACCAGGTTGAC, reverse primer: AGTAGCCAGTTGAAGGAATCAG; WB primary antibody clone F-5, 1 in 1000 dilution Santa Cruz, sc-166561), SERPINB1 (qRT-PCR forward primer: AGGTGTGCAGGATCTCTTTAAC, reverse primer: CCTCTGTTCCCTCTTCATTAC WB primary antibody clone 4D7, 1 in 1000 dilution, Santa Cruz, sc-293462), SERPINB6 (qRT-PCR forward primer: GGTTCTGGTGAATGCTGTCTAT, reverse primer: GCACAGGTTTCTCCTCATTCT; WB primary antibody clone E-8, 1 in 1000 dilution Santa Cruz, sc-398487) and SERPINB13 (qRT-PCR forward primer: CGATGGCCTGGAGAAGATAATAG, reverse primer: CAAGTGCAGATTCACCTTTCTTT; primary antibody clone B29, 1 in 1000 dilution Millipore-Sigma, MABS1320). Transcript levels for HT3^{B3-WT} and SW756^{B3-WT} and the HT3^{B3-KO} and SW756^{B3-KO} clones expressed in 2^{-ΔCt}. Relative intensities compared to actin-HRP (1 in 1000 dilution) for WB are located below gel. Asterix's indicate actin blots that were stripped and reprobred for SERPINB13. Note, some of the actin blots are duplicated Fig S12 as they were stripped and reprobred for cathepsin primary antibodies.

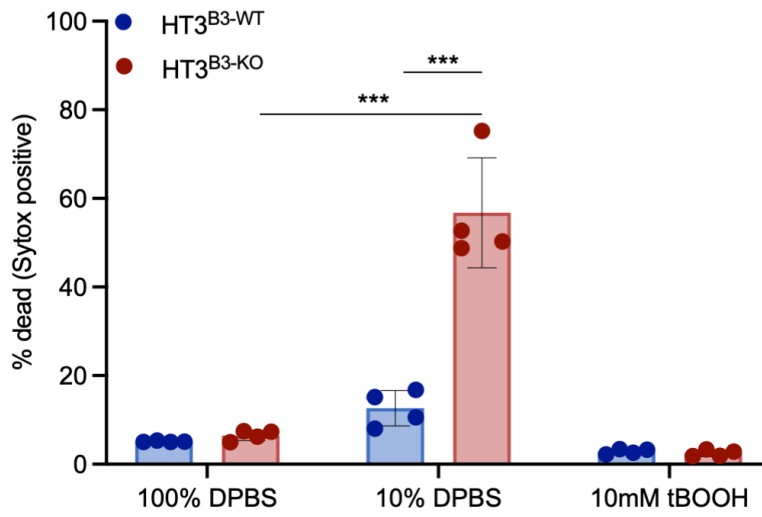


Supplementary Figure 9. Examples of quadruple fluorescent labeled lysosome imaging using for quantification in HT3^{B3-WT} and HT3^{B3-KO} cell lines treated with hypotonic stress. (a-ddd) Representative maximum intensity projections of HT3^{B3-WT} (a-bb) and HT3^{B3-KO} (cc-ddd) cell lines stained with 3 kDa Cascade blue (3K; blue; a-g; cc-ii), 10 kDa Alexa488 (10K; green; h-n; jj-pp), 40 kDa TMR (40K; red; o-u; qq-ww) and 70 kDa Texas red (70K; white; v-bb; xx-ddd) conjugated dextrans prior to exposure to 10% DPBS. Cells were imaged using live cell resonance scanning confocal microscopy in x, y and z (≥ 20 z-planes) over 6 hours at 37 °C and 5% CO₂.

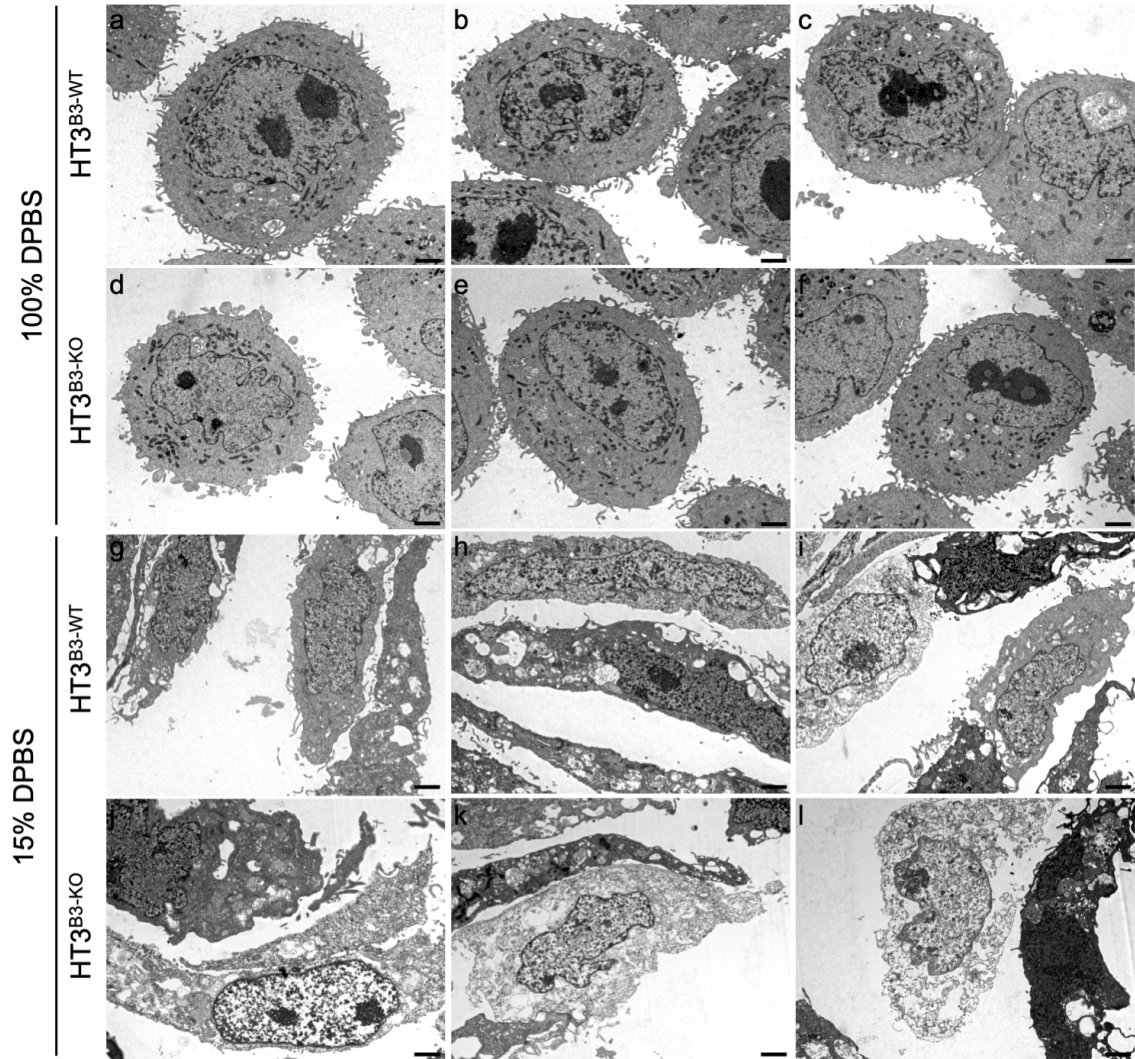
a



b

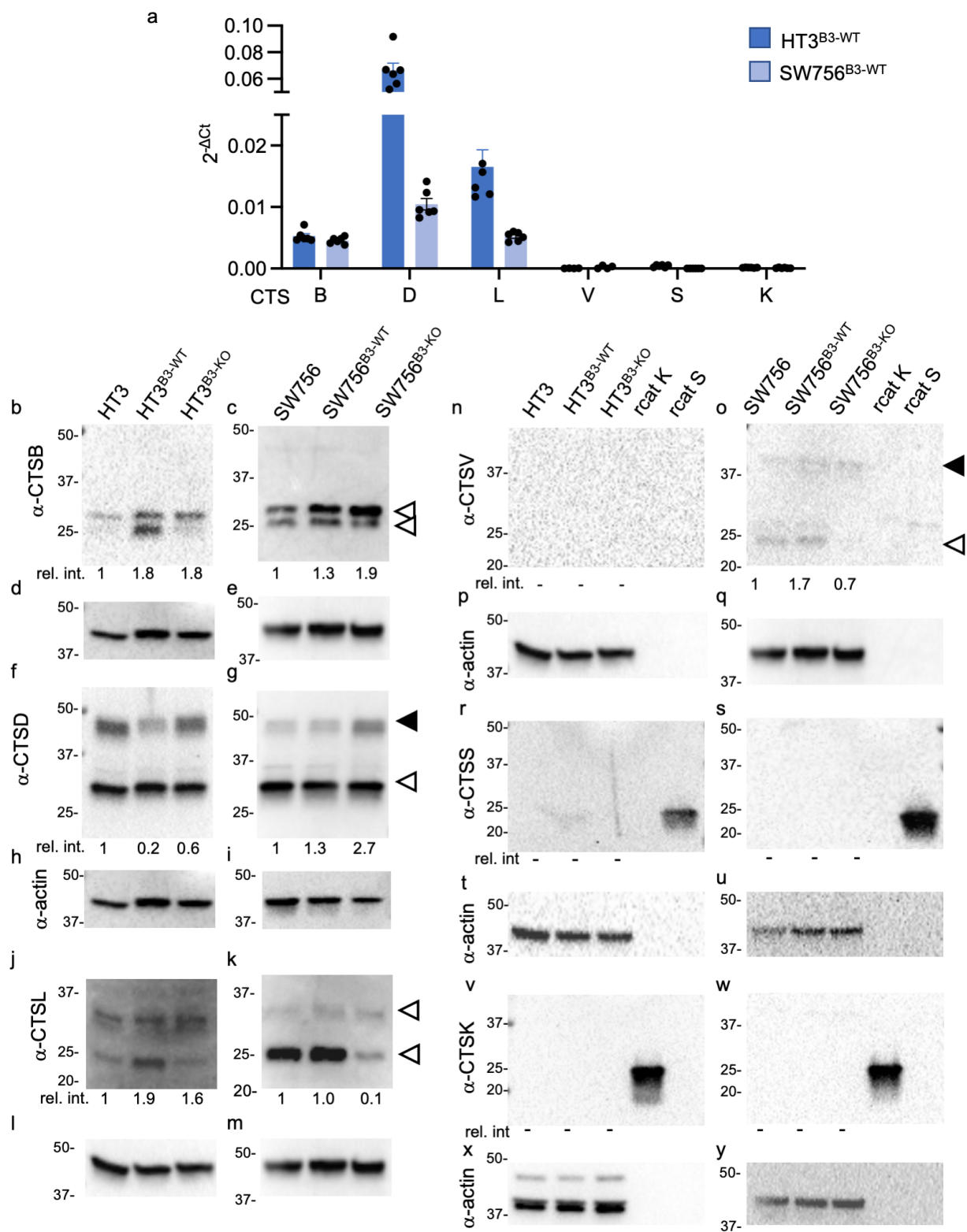


Supplementary Figure 10. Hypotonic stress does not induce ROS in HT3^{B3-WT} or HT3^{B3-KO} cells. A representative experiment of HT3^{B3-WT} and HT3^{B3-KO} cells lines treated with either 100% DPBS (negative control), 10% DPBS or 10 mM *tert*-butylhydroperoxide (tBOOH) (ROS indicator positive control) in the presence of the ROS indicator H2-DCFDA and Sytox orange and imaged using the Cytation 5 at 4 hours at the appropriate wavelengths at 37 °C and 5% CO₂. The total number of cells was calculated using the high contrast brightfield channel. The H2-DCFDA fluorescence intensity was normalized by dividing by the total number of cells (a) and the percent dead was calculated by the number of sytox positive cells/total number of cells × 100 (b). Significance was determined using a two-way ANOVA with Tukeys' multiple comparisons. Note, the significant increase in H2-DCFDA fluorescence intensity in the 10 mM tBOOH positive controls vs the 100% and 10% DPBS treatment.



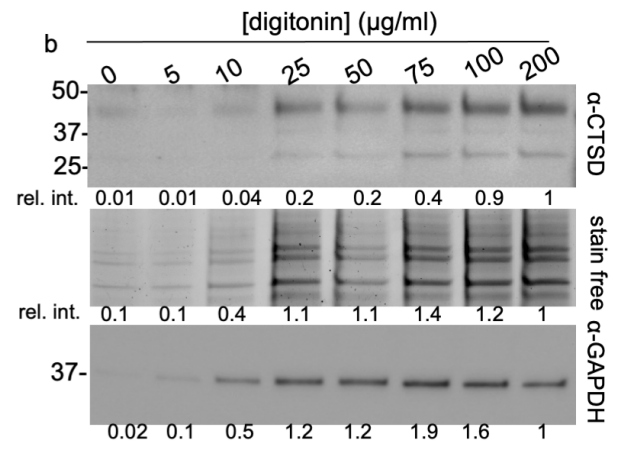
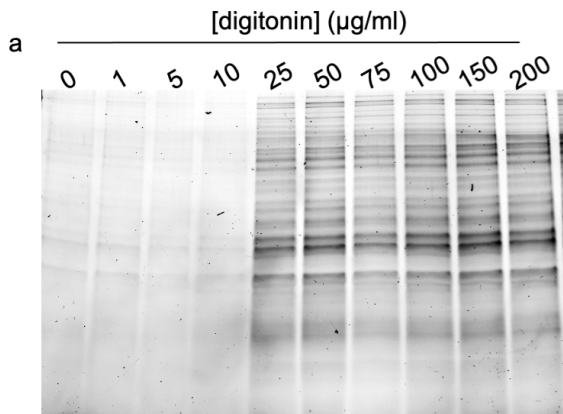
Supplementary Figure 11. Additional transmission electron micrographs from multiple fields of view of HT3 cells treated with hypotonic stress. (a-l)

Additional low power (2000 x magnification) TEM images (scale bars = 2 μ m) of either HT3^{B3-WT} (a-c; g-i) or HT3^{B3-KO} (d-f; j-l) cells treated with either 100% (a-f) or 15% DPBS (g-l) for 4 hours. Note the higher number of cells displaying morphological necrotic cell death characteristics is greater in HT3^{B3-KO} cells treated with 15% DPBS.

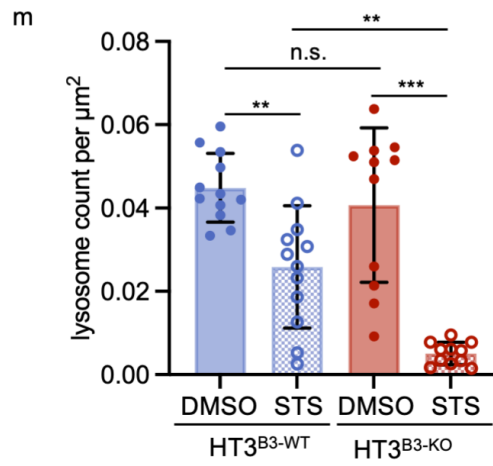
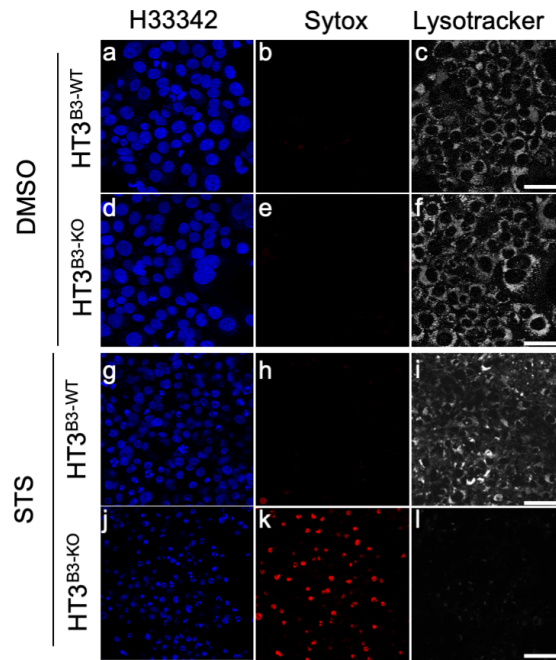


Supplementary Figure 12. HT3 and SW756 cells lines predominantly contain cathepsins B, -D and -L. (a) Quantitative RT-PCR of cathepsin B (CTSB; qRT-PCR forward primer: GAGCTGGTCAACTATGTCAACA, reverse primer: GCTCATGTCCACGTTGTAGAAGT), cathepsin D (qRT-PCR forward primer: TGCTCAAGAACTACAATGGACGC, reverse primer: CGAAGACGACTGTGAAGCACT), cathepsin S (CTSS; qRT-PCR forward primer: AAACGGCTGGTTTGTGTGC, reverse primer: CAGTGGTGATCCAGGGTAGG), cathepsin K (CTSK; qRT-PCR forward primer: ACACCCACTGGGAGCTATG, reverse primer: GACAGGGGTACTTTGAGTCCA), cathepsin L (CTSL; qRT-PCR forward primer: CTTTTGCCTGGGAATTGC, reverse primer: CATCGCCTTCCACTTGGTC) and cathepsin V (CTSV; qRT-PCR forward primer: GGAAGTAAGGAAGGGTGAGATAG, reverse primer: CCTCTAGTATGATGCCCAAGTG), cathepsin S (CTSS; qRT-PCR forward primer: AAACGGCTGGTTTGTGTGC, reverse primer: CAGTGGTGATCCAGGGTAGG), cathepsin K (CTSK; qRT-PCR forward primer: ACACCCACTGGGAGCTATG, reverse primer: GACAGGGGTACTTTGAGTCCA). Transcript levels for HT3^{B3-WT} and SW756^{B3-WT} clones expressed in 2^{-ΔCt}. (b-y) Western blot analysis of the levels of CTSB (b, c), CTSD (f, g), CTSL (j, k), CTSV (n, o), CTSS (r, s) and CTSK (v, w) for HT3 parental cell line (HT3), HT3^{B3-WT}, HT3^{B3-KO} (b, f, j, n, r, & v), SW756 parental cell line (SW756), SW756^{B3-WT} and SW756^{B3-KO} (c, g, k, o, s & w). Black arrowheads denote inactive pro-domain containing forms of the proteases and open arrow denote active forms. Relative intensities (rel. int.) compared to actin-HRP and normalized to the corresponding parental cell line (d e, h, i, l, m, p, q, t, u, x & y) for WB are located below gel. Note, the following actin blots are for the same lysates from blots that was stripped and reprobod:

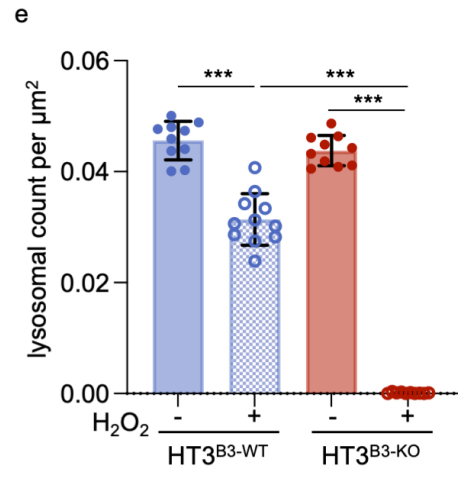
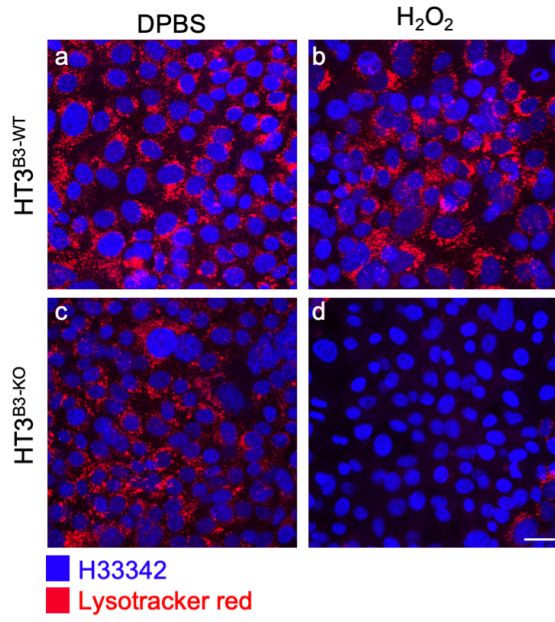
Figs S8d, S12d and S12h; Figs S8h, S12l and S12p; Figs S8l and S12x; S8i, S12e, S12m and S12q; Figs S8q and S12u; Figs S8m and S12y. These blots were duplicated below their corresponding blots for clarity.



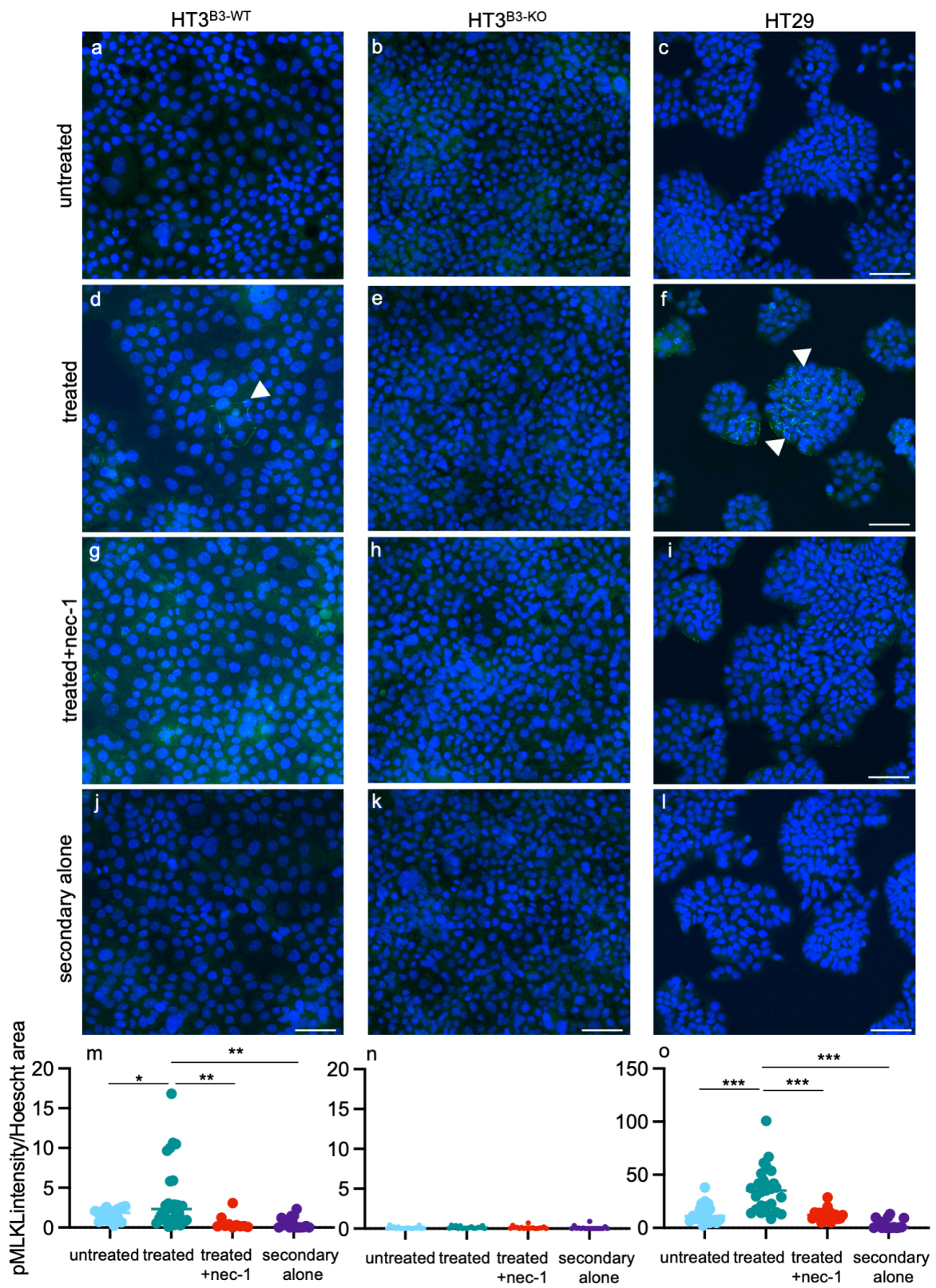
Supplementary Figure 13. Digitonin can specifically release cytoplasmic contents at low concentrations in HT3 cell line. Determination of digitonin concentration that releases cytosolic content without disrupting lysosomes. (a) Stain-free 4-16% gradient SDS-PAGE (Bio-Rad) of supernatants from HT3^{B3-KO} cells treated with the indicated concentration of digitonin for 30 minutes at 4°C in DPBS. Note the increase in total protein release at ≥ 25 $\mu\text{g/ml}$ digitonin concentration. (b) Western blot analysis of lysosomal CTSD and cytosolic GAPDH with corresponding stain free SDS-PAGE of supernatants from HT3^{B3-KO} cells treated with the indicated concentration of digitonin for 30 minutes at 4°C. The background subtracted relative band intensities (rel. int.) for each lane were calculated (Image Lab, v6.1, Bio-Rad) and normalized to the highest concentration of digitonin (200 $\mu\text{g/ml}$).



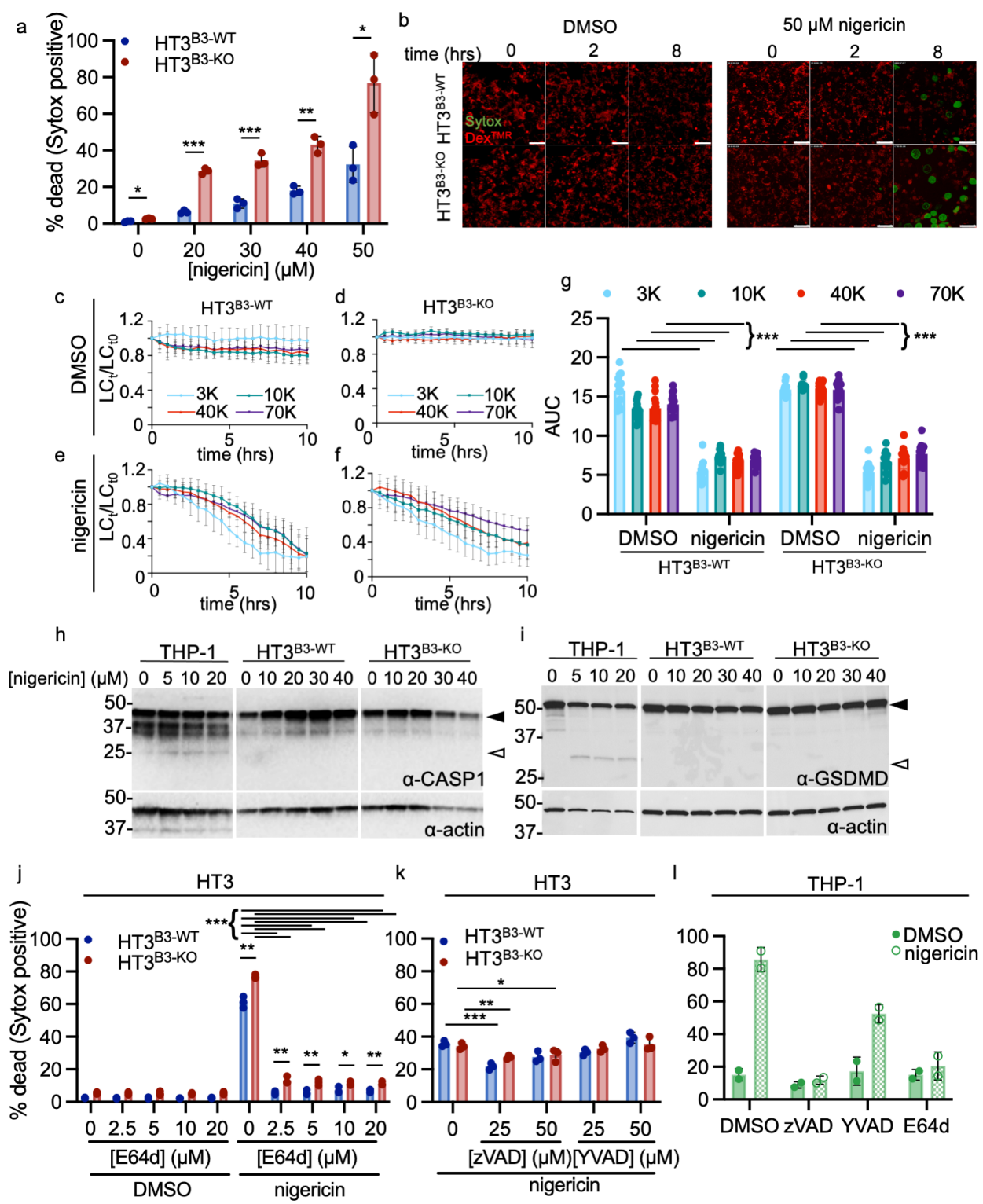
Supplementary Figure 14. HT3^{B3-KO} cells lose Lysotracker™ staining after exposure to staurosporine. (a-l) Representative confocal images of HT3^{B3-WT} and HT3^{B3-KO} cells treated with DMSO control or 5 μ M STS for 16 hours and stained with H33342 (blue), Sytox Orange (red) and lysotracker deep red (white). Scale bars represent 25 μ m. (m) Quantification of the lysotracker positive vesicles (lysosomal count) per μ m² of cellular area in confocal images (shown in panels a-l) of HT3^{B3-WT} (blue bars) or HT3^{B3-KO} (red bars) cell lines were treated with either DMSO (solid fill) or STS (patterned fill) over multiple fields of view ($n \geq 10$). Analyses were compared using an ordinary one way ANOVA with Tukeys' multiple comparisons (** $P < 0.01$, *** $P < 0.001$).



Supplementary Figure 15. HT3^{B3-KO} cells have decreased Lysotracker red staining with H₂O₂ treatment. (a-d) Representative maximum intensity projections of either HT3^{B3-WT} (a-b) or HT3^{B3-KO} (c-d) cells treated with 5 mM H₂O₂ for 8 hours. Cells were stained with H33342 (blue) and Lysotracker Red (red) prior to imaging over x, y and z at multiple fields of view (n ≥ 10) using confocal microscopy. Scale bar represents 25 μm. Note the almost complete loss of lysosomal staining observed in the HT3^{B3-KO} cells treated with H₂O₂ (d). (e) Quantification of the lysotracker positive vesicles (lysosomal count) per μm² of cellular area in HT3^{B3-WT} (blue bars) or HT3^{B3-KO} (red bars) cells treated with H₂O₂ (+; patterned fill) or the equivalent volume of DPBS (-; solid fill) over multiple fields of view (n ≥ 10, *** *P* < 0.001, two-tailed *t*-Test).

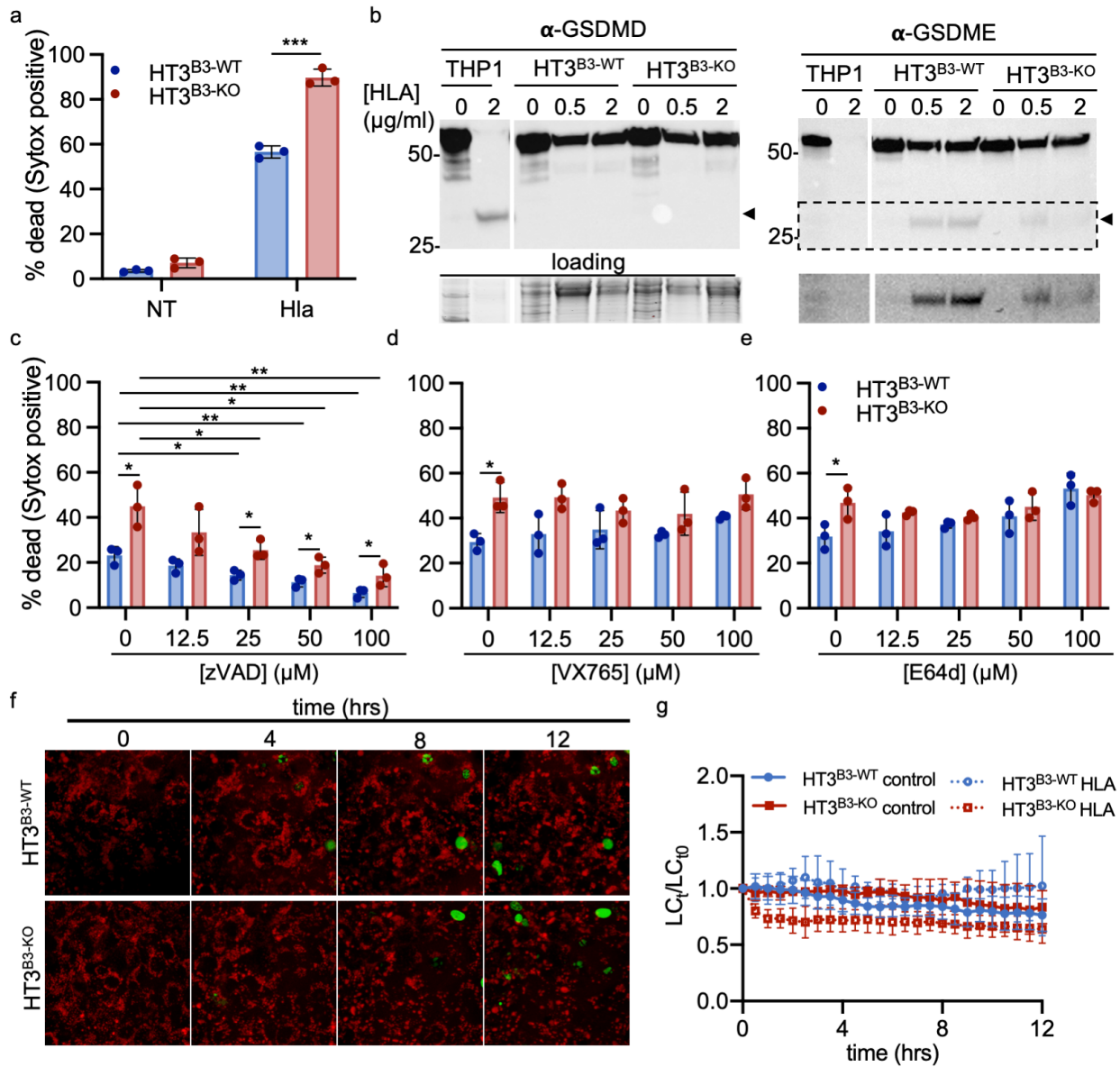


Supplementary Figure 16. pMLKL can be induced in HT3^{B3-WT} cells treated with necroptosis inducers. (a-l) Representative confocal images of HT3^{B3-WT} (a, d, g, j), HT3^{B3-KO} (b, e, h, k) and HT29 (positive control; c, f, i, l) cell lines treated with diluent (untreated; a-c) TNF α + BV6 + qVD-OPh + cyclohexamide (HT3 cells) or TNF α + zVAD-fmk (HT29) (treated; d-f), the same treatments but in the presence of 10 μ M necrostatin-1 (treated+nec-1, g-i) for 8 hours prior to fixation and immunofluorescence detection of phospho-MLKL (green) and counterstained with Hoescht 33342 (blue). As a background fluorescence control, the primary phospho-MLKL was omitted from staining in a subset of untreated cells (secondary alone, j-l). White arrowheads indicate areas of phospho-MLKL plasma membrane staining. (m-o) Quantification of multiple fields of the phospho-MLKL staining fluorescence above background normalized to the number of cells imaged as indicated by the total Hoescht 33342 area (pMLKL intensity/Hoescht area) over $n \geq 10$ separate fields per treatment. Statistical significance was determined using a two-way ANOVA with Tukeys' multiple comparisons (* $P < 0.05$, ** $P < 0.01$, *** $P < 0.001$). Note, the statistically significant increase in pMLKL intensity/Hoescht area between HT3^{B3-WT} and HT29 untreated and treated samples that was abrogated with nec-1 treatment.



Supplementary Figure 17. Nigericin does not induce pyroptosis in HT3 cells but does induce LMP. (a) Either HT3^{B3-WT} (blue bars) or HT3^{B3-KO} (red bars) cells were incubated with the indicated concentration of nigericin for 24 hours at 37°C / 5% CO₂ in the presence of Sytox Orange. Cells were stained with H33342 and the percent dead was calculated as (# Sytox positive nuclei/# of blue nuclei) × 100. The means ± SD of a representative experiment were compared using a two-tailed *t*-test (****P* < 0.001, ***P* < 0.01, * *P* < 0.05). Note that at all concentrations of DMSO there is a statistical increase in % dead in the HT3^{B3-KO} cells. (b) Representative maximum intensity projections of either HT3^{B3-WT} or HT3^{B3-KO} labeled with 10kDa TMR-dextran (red) and exposed to DMSO diluent control or 50 μM nigericin in the presence of Sytox Green (green). Cells were imaged by live-cell time lapse confocal microscopy in X, Y, Z at multiple fields of view. The indicated time points are shown. Scale bars represent 25 μm. Note the loss of lysosomal staining in both cell lines but an increase in Sytox Green staining in HT3^{B3-KO}. (c-f) To quantify lysosomal content, HT3^{B3-WT} or HT3^{B3-KO} cells were incubated with fluorescently labeled different molecular weight dextrans as previously stated, treated with either diluent control (DMSO) or 50 μM nigericin at multiple positions (fields ≥ 10) over 10 hours at 37°C and 5% CO₂ and imaged using live-cell confocal microscopy. Number of lysosomes at each time point (LC_t) were normalized to the lysosome count at time zero (LC_{t0}). (g) AUC for each dextran over time for experiment in c-f (compared by 2-way ANOVA with Tukey's multiple comparisons test). (h-i) Western blot analysis of caspase-1 (CASP1) or gasdermin D (GSDMD) cleavage and actin protein levels from LPS pretreated THP-1, HT3^{B3-WT} and HT3^{B3-KO} cell lysates after exposure to the indicated concentrations of

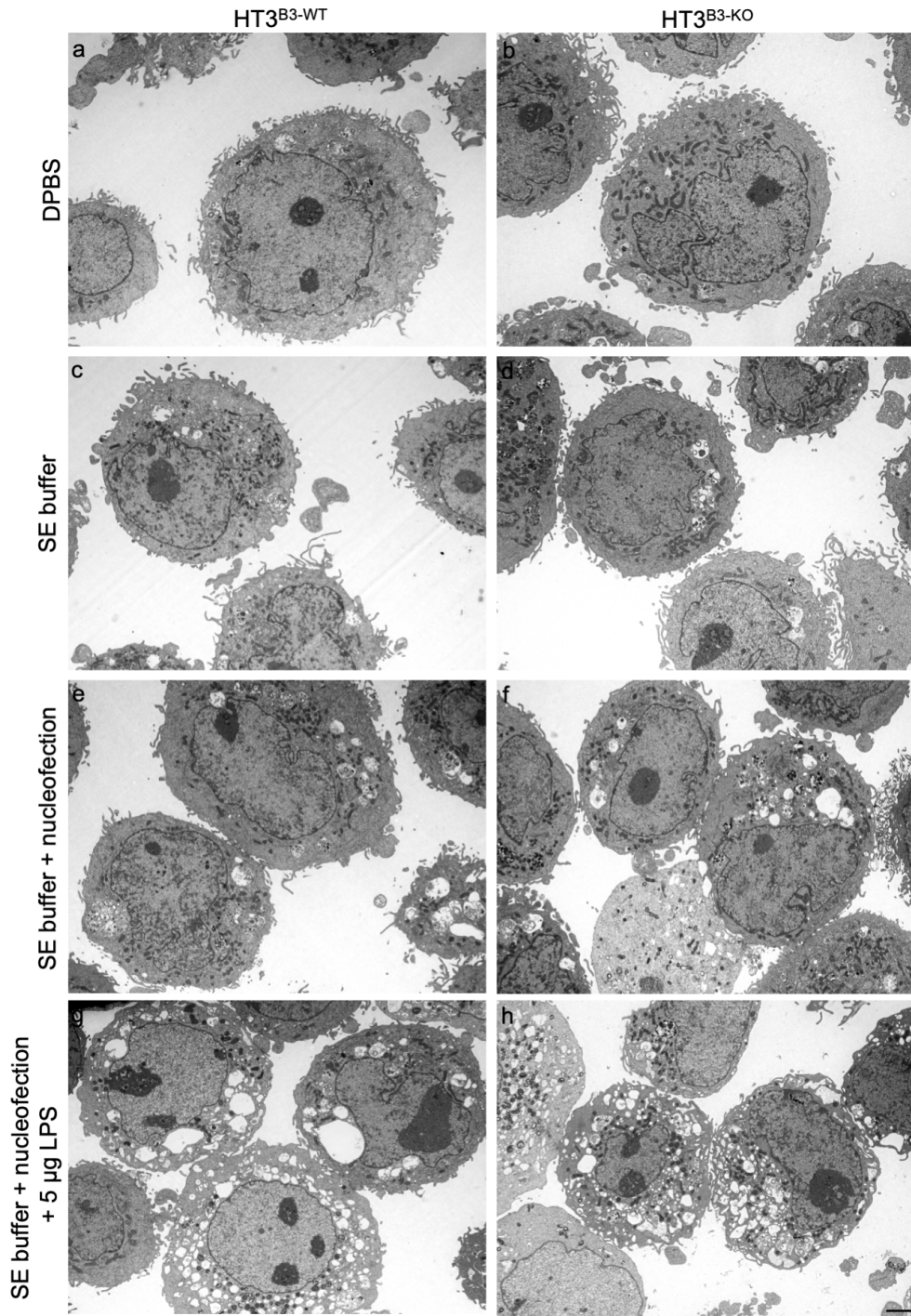
nigericin for 5 hours. Note the presence of P25 and P30 cleavage band (open arrowhead) in the THP-1 cell line for CASP1 and GSDMD, respectively. There was no detectable cleavage of CASP1 or GSDMD in the HT3 cell lines. (j, k) Either HT3^{B3-WT} (blue bars) or HT3^{B3-KO} (red bars) cells were incubated with the indicated concentration of E64d (j), z-VAD-fmk and YVAD-CHO (k) for 1 hour at 37°C / 5% CO₂ in the presence of Sytox Orange. Cells were then incubated with diluent control (DMSO) or 50 µM nigericin for 16 hours and stained with H33342. The percent dead was calculated as (# Sytox positive nuclei/# of blue nuclei) × 100. The means ± SD of a representative experiment were compared using a two-tailed *t*-test (****P* < 0.001, ***P* < 0.01, **P* < 0.05). Notably, the protection in both HT3 cell lines treated with E64d with little protection with z-VAD-fmk and no protection of YVAD-CHO. (l) THP-1 (green bars) cells were incubated with 1 µg / ml LPS and 50 µM of the indicated inhibitor for 3 hours at 37°C / 5% CO₂. Cells were then treated with DMSO diluent control (solid fill) or 10 µM nigericin (pattern fill) for 2 hours in the presence of Sytox Orange. Prior to imaging, cells were stained with H33342 and the percent dead was calculated as (# Sytox positive nuclei/# of blue nuclei) × 100. The means (n = 2) ± SD of a representative experiment are shown. Notably, the protection from Sytox staining was observed with z-VAD-fmk, YVAD-CHO and E64d.



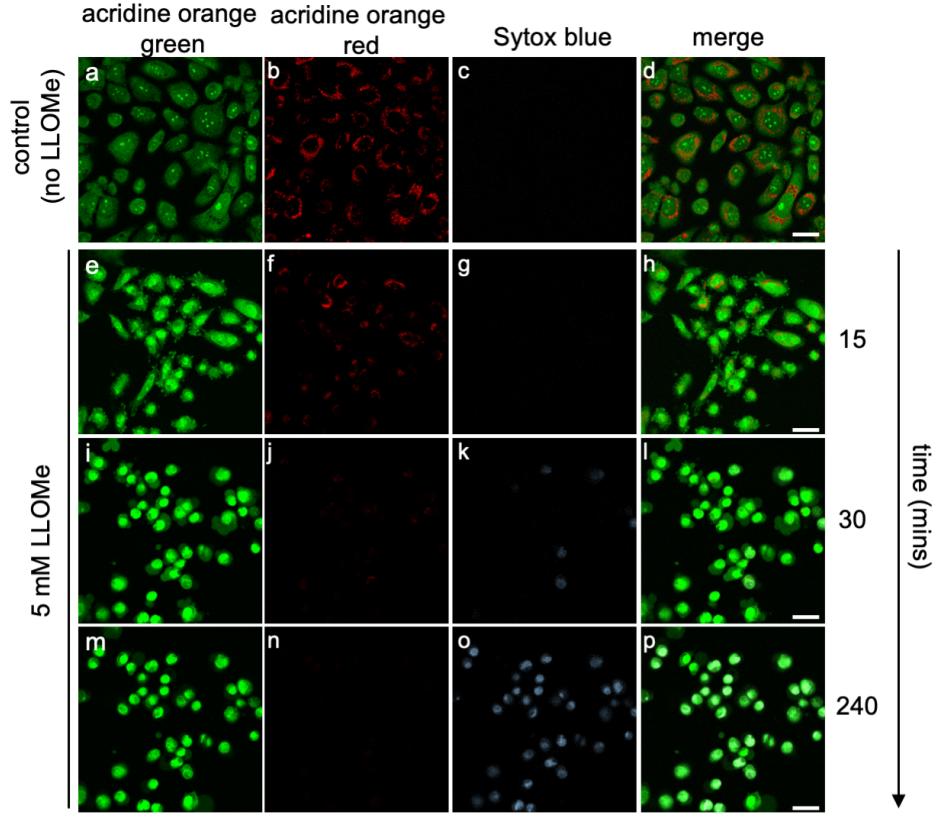
Supplementary Figure 18. Alpha hemalysin induces gasdermin E cleavage

in HT3 cells. (a) Either HT3^{B3-WT} (blue bars) or HT3^{B3-KO} (red bars) cells were incubated without (NT) or with 1 µg / ml of alpha hemalysin (Hla) for 24 hours at 37°C / 5% CO₂ in the presence of Sytox Orange. Cells were stained with H33342 and the percent dead was calculated as (# Sytox positive nuclei/# of blue nuclei) × 100. The means ± SD of a representative experiment were compared using a two-tailed *t*-test (***P*<0.001). (b) Western blot analysis of gasdermins D (GSDMD) and E (GSDME) in THP-1, HT3^{B3-WT} or HT3^{B3-KO} cells treated with the indicated HLA concentration for 1.5 hours after LPS pretreatment for THP-1 cells and 16 hours for HT3 cell lines. Cell lysates were separated by SDS-PAGE and GSDMD and GSDME detected using the appropriate mAb. GSDMD and GSDME cleavage products are indicated by the black arrowheads. Hashed box in GSDME blot indicates the enhanced area below the gel. Numerals indicate the molecular weight markers in kDa. Total protein loading was indicated by stain free SDS-Page (BioRad). Note the presence of a GSDME band in HT3 cell lines absent in THP-1 cells and no detectable cleavage of GSDMD. (c-e) Either HT3^{B3-WT} (blue bars) or HT3^{B3-KO} (red bars) cells were incubated with the indicated concentration of z-VAD-fmk (c), caspase-1 inhibitor, VX735 (d) and E64d (e) for 3 hours prior to treatment with 1 µg / ml Hla at 37°C / 5% CO₂ for 18 hours. Cells were stained with H33342 and the percent dead was calculated as (# Sytox positive nuclei/# of blue nuclei) × 100. The means ± SD of a representative experiment were compared using a two-tailed *t*-test (***P*<0.01, * *P*<0.05). Note that protection was only observed in z-VAD treated cells. (f) Representative maximum intensity projections of either HT3^{B3-WT} or HT3^{B3-KO} cells were labeled with 10 kDa TMR-

Dextran and imaged by time-lapse live cell confocal microscopy in X, Y, Z over multiple fields with 1 μg / ml Hla in the presence of Sytox Green over 12 hours. Note the lack of lysosomal loss in both HT3 cell lines. (g) Quantification of the lysosomal count at each time point of the images shown in F normalized to time 0. HT3^{B3-WT} (blue lines, circles) or HT3^{B3-KO} (red lines, squares) cells were not treated (control, filled symbols) or treated with 1 μg / ml Hla (dashed lines, open symbols) prior to imaging. Representative experiment over $n \geq 7$ fields.

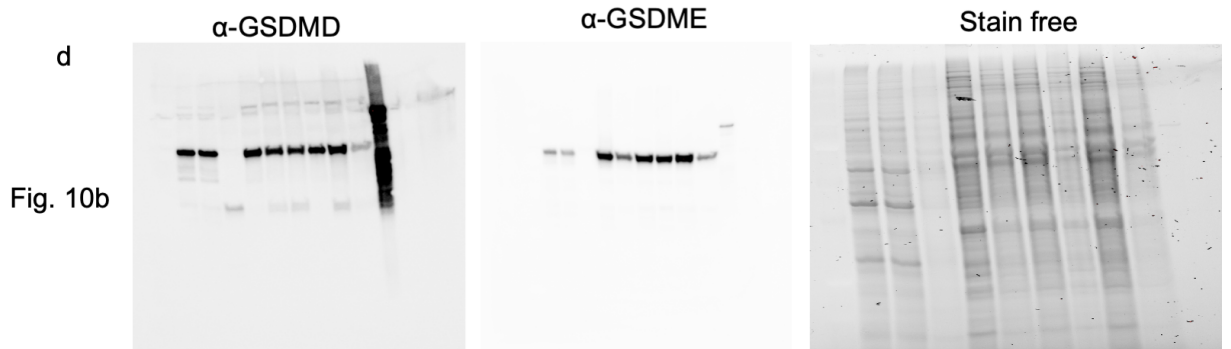
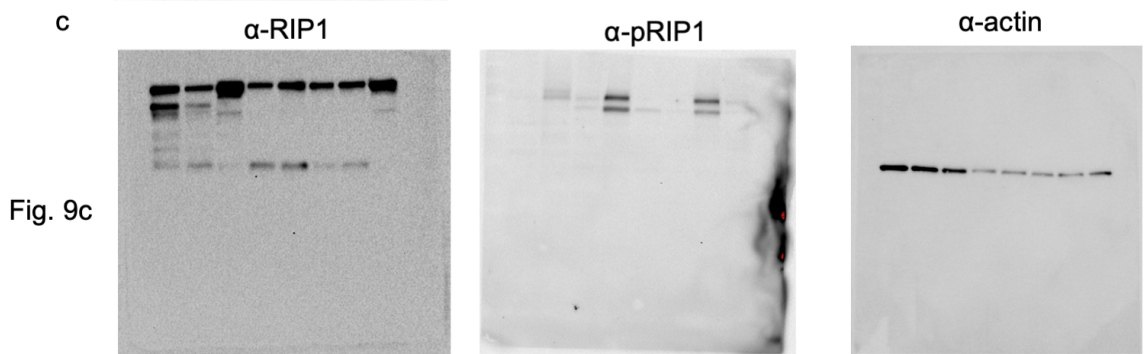
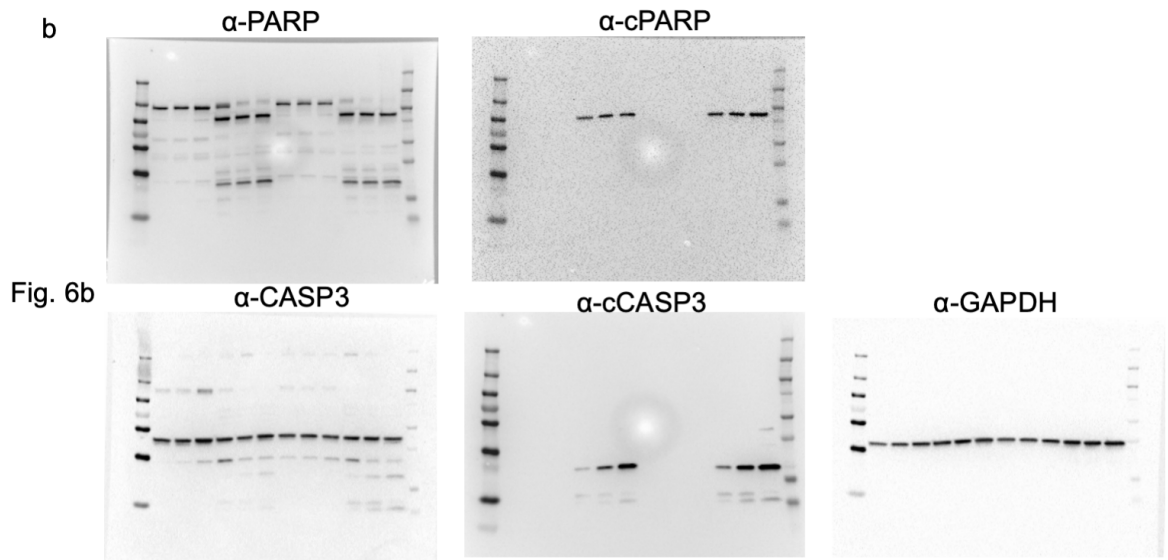
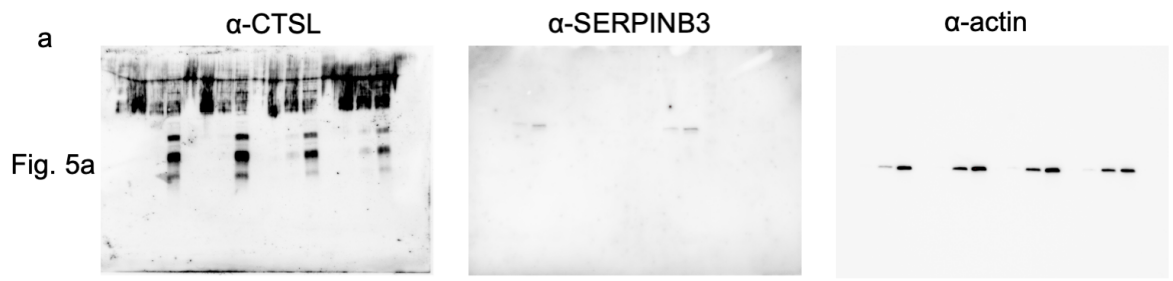


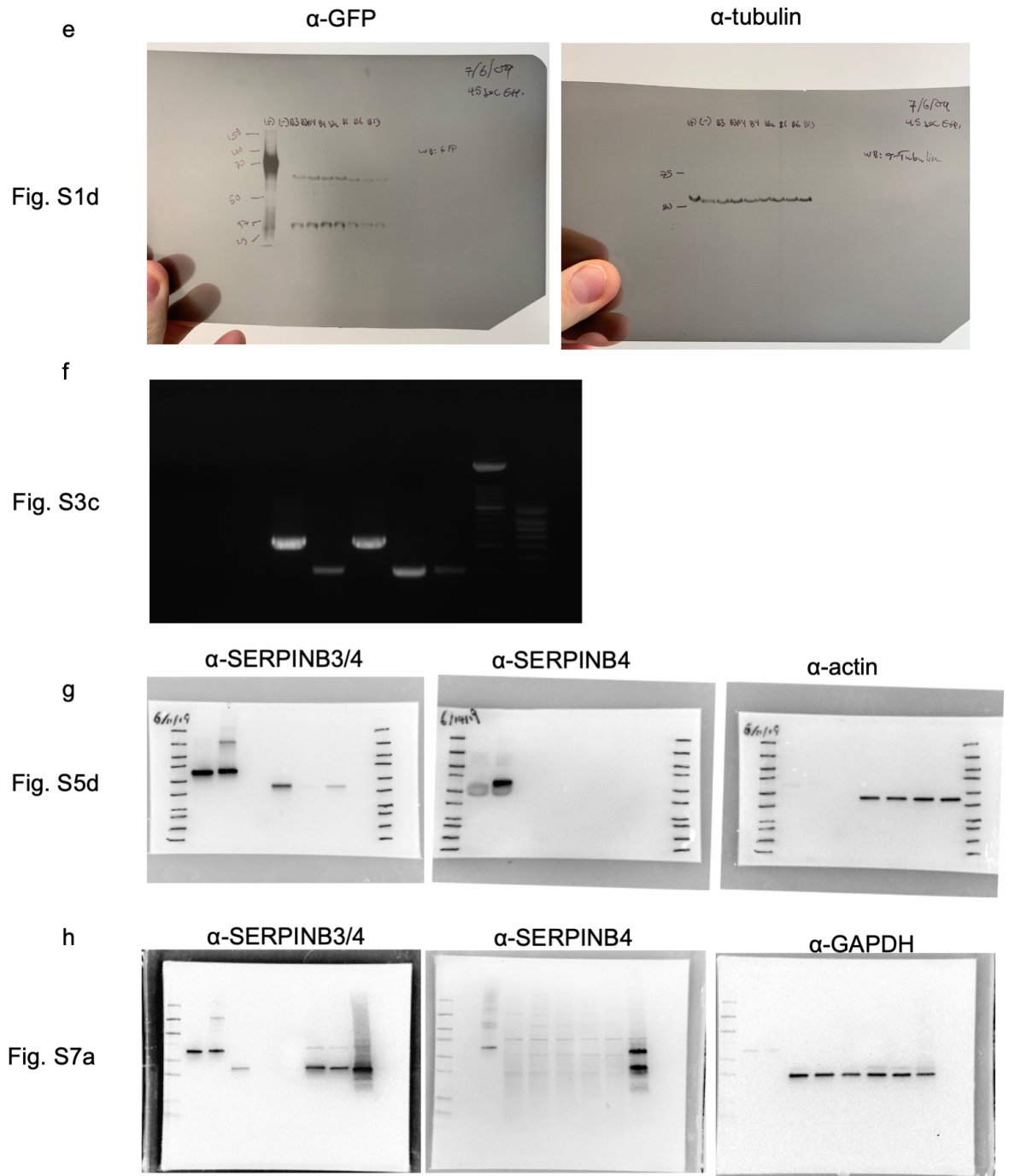
Supplementary Figure 19. LPS^{cyto} induces cytoplasmic vacuolization in both HT3^{B3-WT} and HT3^{B3-KO} cells. (a-h) Representative low power (2000x) TEM images of either HT3^{B3-WT} (a, c, e, g) or HT3^{B3-KO} (b, d, f, h) cells treated with DPBS (a, b), SE nucleofection buffer only (c, d), SE buffer plus nucleofection without LPS (e, f) and SE buffer plus nucleofection with 5 µg of LPS (g, h). All cells were allowed to recover in media for 2 hours. Scale bar represents 2 µm. Note the presence of cytoplasmic vacuoles in both HT3 cell lines.



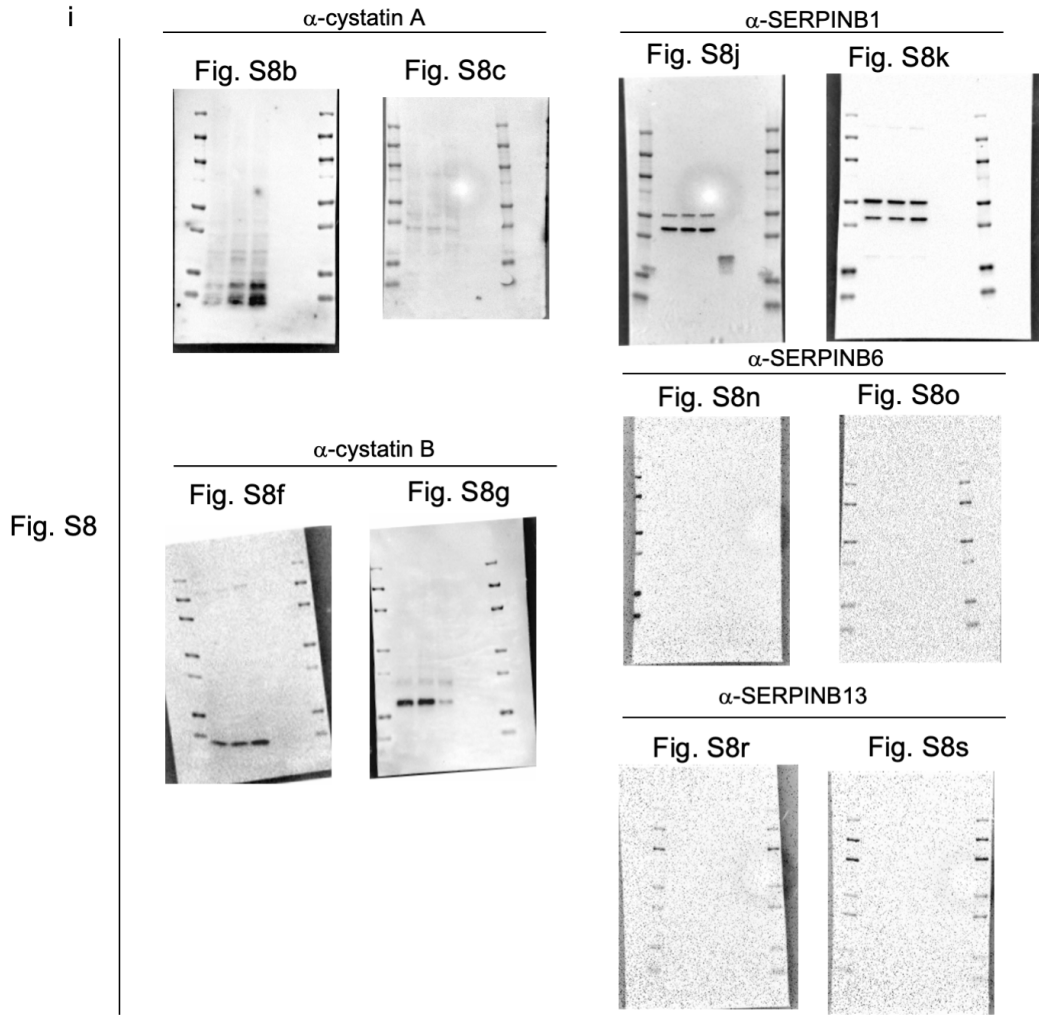
Supplementary Figure 20. LLOMe induces lysosomal membrane

permeabilization in HT3 cells. (a-p) Representative confocal images of HT3^{B3-WT} cells labeled with acridine orange and Sytox blue and imaged using excitation lasers 405 nm (blue; c, g, k, o), 488 nm (green; a, e, i, m) and 561 nm (red; b, f, j, n) in x, y, z over time. A merge of all channels is also shown (d, h, l, p). Cells were imaged prior to the addition of LLOMe (-a-d) and then at the indicated time points after the addition of 5 mM LLOMe (e-p). Scale bars represent 25 μ m. Note the loss of red acidic vesicles with LLOMe treatment.





i



j

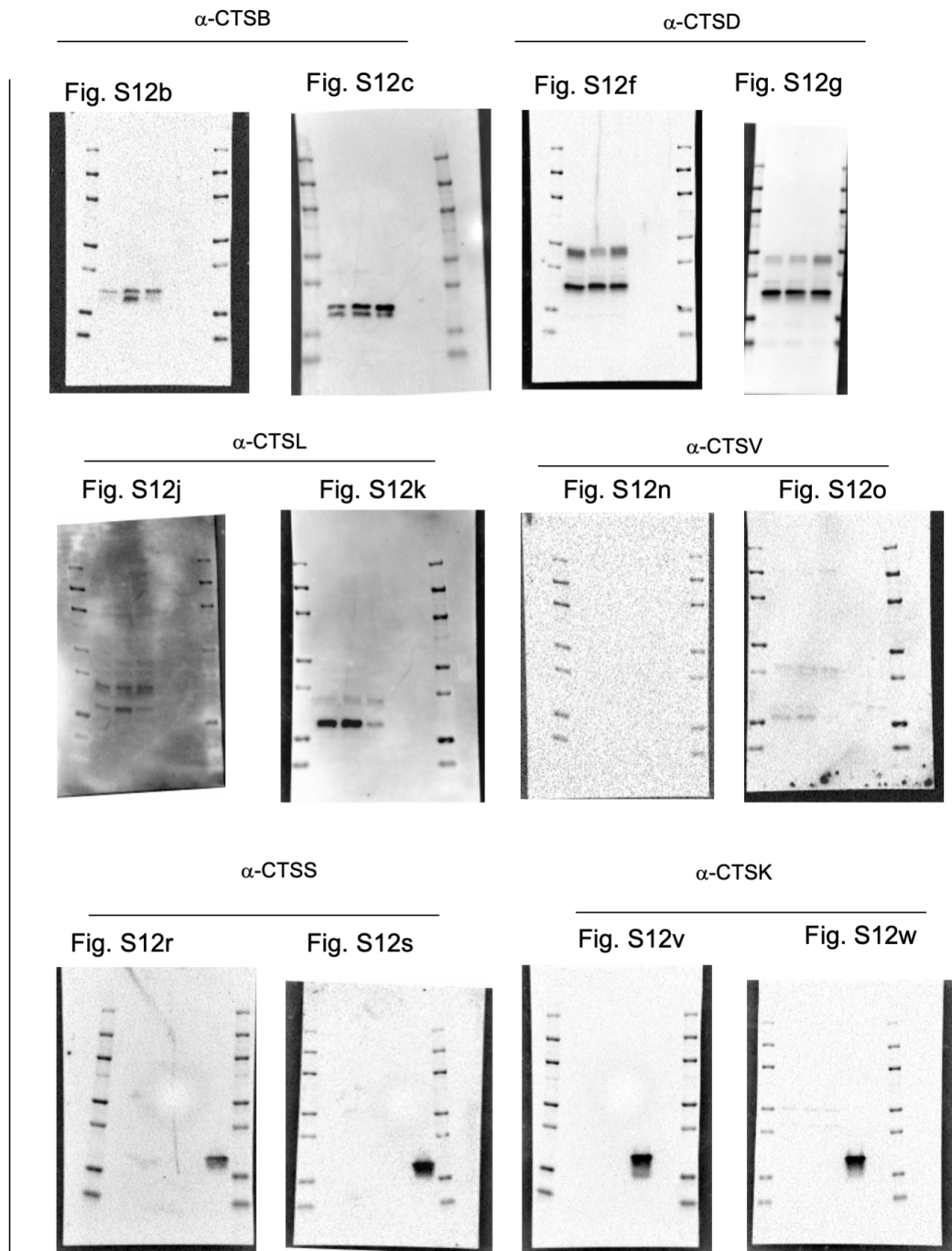


Fig. S12

k

Figs. S8d, S12d & S12h

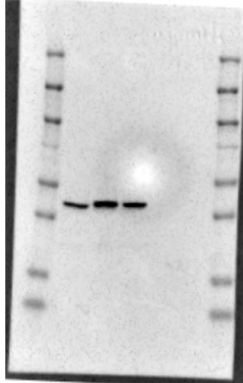
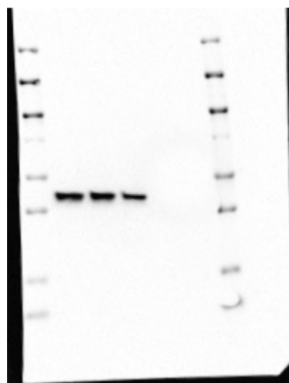
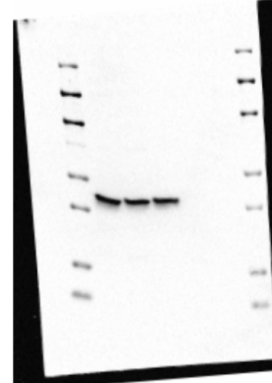


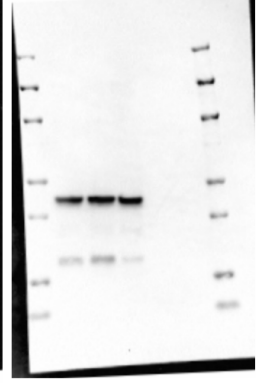
Fig. S8e



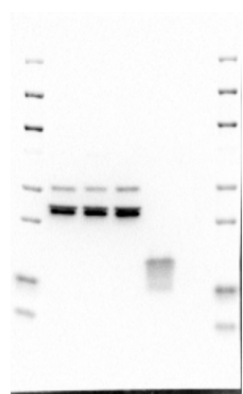
Figs. S8h, S12l & S12p



Figs. S8i, S12e, S12m & S12q



Figs. S8l & S12x



Figs. S8m & S12y

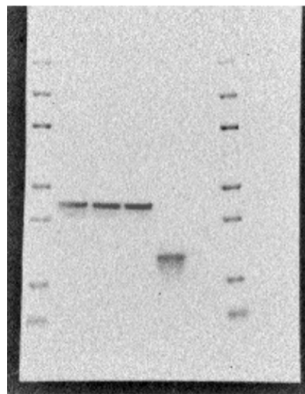
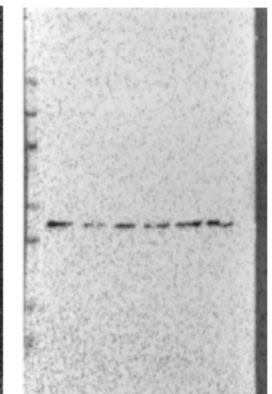
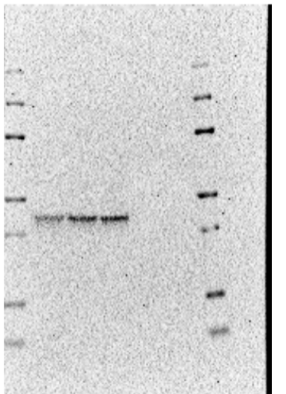


Fig. S8p



Figs. S8q & S12u



Figs. S8 and S12 actin blots

Fig. S12i

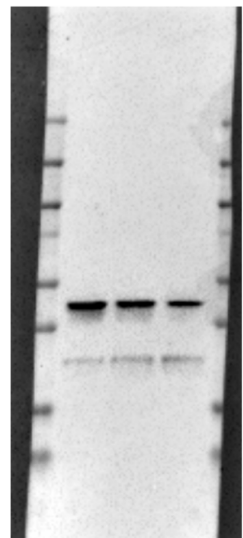
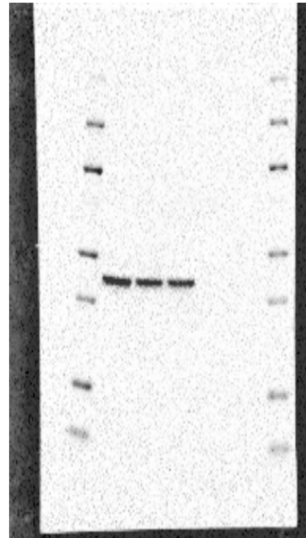
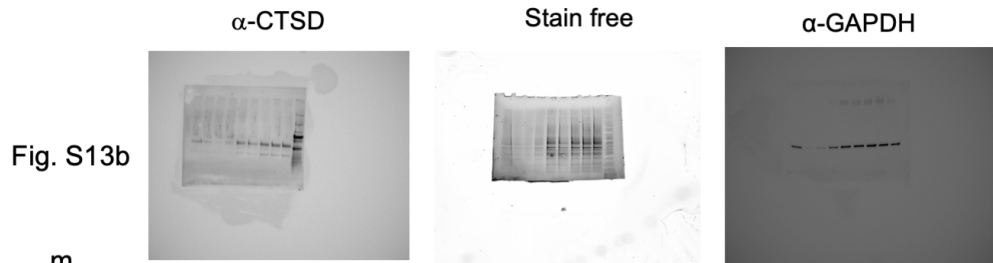
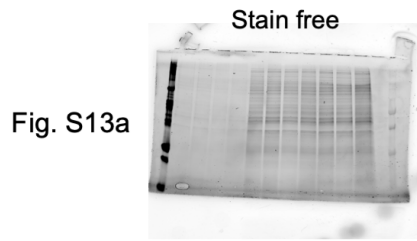


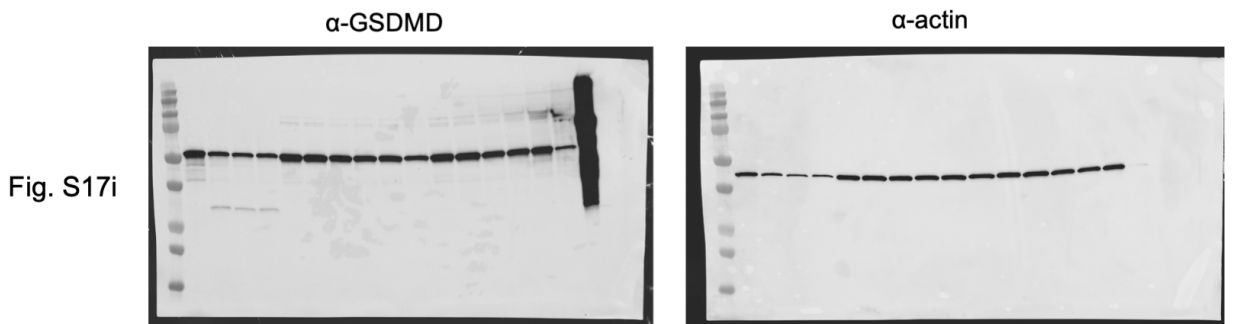
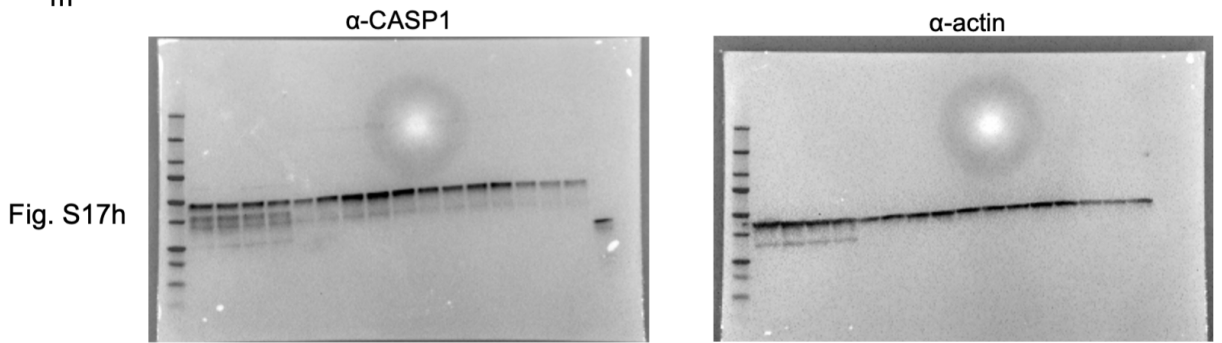
Fig. S12t



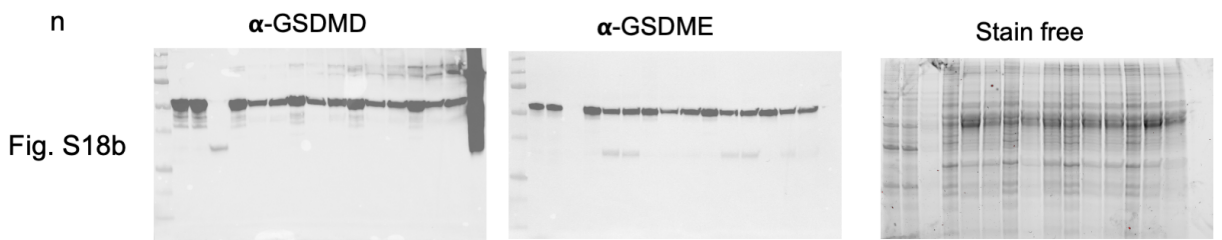
l



m



n



Supplementary Figure 21. Uncropped immunoblots and gel images from data used in this manuscript. (a-n) Uncropped images from Figures 5 (a), 6 (b), 9 (c), 10 (d), S1 (e), S3 (f), S5 (g), S7 (h), S8 (i, k), S12 (j, k), S13 (l), S17 (m) and S18 (n). The antibodies or stains used are indicated above the individual images. The corresponding figure panels are denoted on the left.